

USR# 15694

~~CONFIDENTIAL~~

195  
Copy  
RM E54H10

NACA RM E54H10

0144000

TECH LIBRARY KAFB, NM

NACA

# RESEARCH MEMORANDUM

9689

## PRELIMINARY REPORT OF EXPERIMENTAL INVESTIGATION OF RAM-JET CONTROLS AND ENGINE DYNAMICS

By G. Vasu, F. A. Wilcox, and S. C. Himmel

Lewis Flight Propulsion Laboratory

Cleveland, Ohio (Unclassified...)

NASA Tech Pub Announcement H-11  
(NOT AUTHORIZED TO CHANGE)

21 Jan 60

NK

GRADE OF OFFICER MAKING CHANGE)

23 Feb 61

DATE

CLASSIFIED DOCUMENT

This material contains information affecting the National Defense of the United States within the meaning of the espionage laws, Title 18, U.S.C., Secs. 793 and 794, the transmission or revelation of which in any manner to an unauthorized person is prohibited by law.

NATIONAL ADVISORY COMMITTEE  
FOR AERONAUTICS

WASHINGTON

October 25, 1954

~~CONFIDENTIAL~~



0144000

NACA RM E54H10

~~CONFIDENTIAL~~

## NATIONAL ADVISORY COMMITTEE FOR AERONAUTICS

RESEARCH MEMORANDUMPRELIMINARY REPORT OF EXPERIMENTAL INVESTIGATION OF  
RAM-JET CONTROLS AND ENGINE DYNAMICS

By G. Vasu, F. A. Wilcox, and S. C. Himmel

60709

CK-1

SUMMARY

The preliminary results of an experimental investigation of the internal dynamics of a ram-jet engine and the steady-state and dynamic performance characteristics of a number of ram-jet engine controls are presented. The investigation was conducted on a 16-inch ram-jet engine over the range of free-stream Mach numbers from 1.5 to 2.16.

Three types of engine control system were investigated. These were (1) shock positioning, (2) direct control of diffuser-exit pressure, and (3) an optimalizing control designed to obtain peak pressure recovery from the diffuser. All three systems operated satisfactorily and appear to present practicable means of controlling ram-jet engines.

The responses of pressures within the ram-jet engine to disturbances in fuel flow appear to comprise a dead time in cascade with a lead-lag characteristic. The dead time varied from 0.02 to 0.05 second over the range of engine and simulated flight conditions investigated. The rise ratio in the lead-lag characteristic varied from 0.5 to 1.0, and the time constant in the lead-lag varied from 0.1 to 0.4 second over the same range of conditions.

INTRODUCTION

The successful application of the ram-jet engine as a propulsion system for supersonic flight is dependent, to a great extent, upon the development of engine control systems capable of maintaining a desired mode of engine operation and minimizing departures from desired conditions resulting from external and internal disturbances acting on the engine-control system.

Prior to the design of a satisfactory control system, two things must be determined: first, the parameters which can be used to control the system; and second, the static and dynamic performance characteristics of the system to be controlled. Analyses (refs. 1 and 2) have

~~CONFIDENTIAL~~

indicated some ram-jet engine parameters which can be used for control purposes and also some of the techniques possible in applying these parameters in control loops.

In order to determine the dynamics of ram-jet engine performance and to ascertain the practicability of several control techniques, an experimental investigation was conducted on a full-scale ram-jet engine in the 8- by 6-foot supersonic wind tunnel of the NACA Lewis laboratory. The objective of the engine dynamics portion of the experimental program was to ascertain the nature of the response of the internal pressures of the ram-jet engine to disturbances of the engine independent variables (fuel flow, angle of attack, Mach number, and exhaust-nozzle area). The controls portion of the program was designed to evaluate the steady-state and dynamic performance characteristics of three different control techniques: (1) shock positioning, (2) direct control of diffuser pressure recovery, and (3) "optimalizer" control of diffuser pressure recovery. The latter two techniques are described in reference 2.

3409

#### APPARATUS AND INSTRUMENTATION

##### Engine and Installation

The engine used in the test program was a 16-inch-diameter ram jet and is shown mounted in the 8- by 6-foot supersonic wind tunnel in figure 1(a). A detailed description of the engine and its performance is given in reference 3.

The inlet was designed so that the oblique shock generated by the 25° half-angle conical spike fell slightly ahead of the cowl lip at the design Mach number of 1.8. The engine had a conical exhaust nozzle with an exit area of 0.69 of the combustion-chamber area. Reductions in exit nozzle area up to 21 percent were obtained by the use of a movable water-cooled plug.

Engine angle of attack could be varied from zero to 10° by rotating the engine about a pivot point in the support strut. By use of the inclined-plate technique described in reference 4, the Mach number of the free stream entering the engine could be varied rapidly by pitching the engine with plates attached to an angle of approximately 5°. Two plates were used; the first provided a range of Mach numbers from 1.7 to 1.9, and the second, from 2.0 to 2.16.

Internal features of the engine are shown in figure 1(b). The engine was equipped with a can-type burner. Engine air flow and diffuser-exit total-pressure recovery were evaluated at station x located 57 inches downstream of the cowl lip. Combustion-chamber-inlet conditions were based on the flow area of station 3. Static-pressure taps used in

shock-positioning controls were located on the horizontal center line of the centerbody, and their locations are tabulated in figure 1(b). Two total-pressure tubes were used for one of the shock-positioning controls; the first was located in the tip of the inlet spike, and the second was on the horizontal center line of the engine slightly outside of the engine cowl. A detail of the latter tube is also shown in figure 1(b).

6072

CK-1 back

### Fuel System

The fuel injection system comprised primary and secondary manifolds located 17 inches upstream of the burner can, as shown in figure 1(b). The primary system contained six nozzles and the secondary contained 16 nozzles. A pilot burner was included in the system and was located just forward of the can. The fuel used throughout the program was MIL-F-5624B, amendment 1, grade JP-4. A servo system was used to control the secondary flow to the engine, it having been ascertained that satisfactory engine operation was possible over the range of test conditions with constant primary fuel flow.

The fuel system controlling the flow to the secondary nozzles is shown schematically in figure 2. The system constitutes an electro-hydraulic servo system which positions a throttle in a specially designed fuel metering valve in response to an input voltage signal. The servo system operates in the following manner: The input voltage  $V_i$  is compared with a position feedback voltage  $V_f$ , and the difference or error voltage is amplified by a d-c amplifier. (All symbols are defined in the appendix.) The output of the amplifier is fed into a torque motor which moves the pistons of a pilot valve porting high-pressure hydraulic fluid to the appropriate side of a hydraulic throttle power servo, which is an integral part of the throttle assembly in the fuel valve. The position of the throttle is sensed by a differential-transformer-type position transducer energized by an oscillator. The output signal of the transducer is amplified, demodulated, and filtered, the output of the filter being the position feedback voltage. The system acts to provide a linear relation between input voltage and throttle position. The design principles used in the design of the throttle power servo are described in reference 5.

The fuel metering valve incorporates a differential relief valve which maintains a constant pressure differential across a metering orifice. Fuel flow, therefore, varies directly with throttle position. The differential relief valve was designed for fast response and stability according to the method described in reference 6.

The steady-state performance of the fuel system is shown in figure 3, where the fuel flow out of the metering valve is shown as a function

of the servo input voltage. The dynamic performance of the system as installed for the test program is shown in figure 4, wherein the frequency-response characteristics of fuel nozzle pressure drop to input voltage are presented. The frequency-response characteristic includes the dynamic effects of all the necessary piping, and so forth, required for the installation. Figure 4 indicates the phase shift and the attenuation that had to be considered in the design of the control loops.

3409

### Instrumentation

For the measurement of engine variables during transient operation of the engine, it was necessary to select instruments having fast response in view of the short response times expected. For the measurement of pressures within the engine, pressure transducers of the variable inductance type having high natural frequencies were selected. Connecting-tubing lengths were kept to a minimum and, wherever possible, static pressures were measured by transducers screwed directly into the static-pressure tap.

Typical frequency-response characteristics of the pressure transducers are shown in figure 5. These data were obtained from bench tests. The static-pressure sensor shows flat frequency response from zero to 300 cycles per second. The total-pressure sensor is slightly underdamped, having a peak amplitude ratio of approximately 1.2 at 100 cycles per second.

Engine pressures were sensed by transducers at the following locations (fig. 1(b)):

Station	Sensor	
	Type	Number
0	Total	1
a	Static	1
b	Static	1
c	Static	1
d	Static	1
x	{ Static	2
	Total	2
3	Static	1
4	Static	1

For steady-state performance, these pressures were measured by manometers.

For the measurement of angle of attack and exit area during transients, slide-wire potentiometers were used. The exit-area indication was obtained by sensing the position of the exit nozzle plug. In steady state these variables were measured by counters.

Fuel nozzle pressure drop was measured by strain-gage-type pressure transducers connected approximately 6 inches upstream of both the primary and the secondary fuel nozzles and referenced to the air pressure in the region. These pressure transducers had flat frequency-response characteristics to at least 50 cycles per second. For steady-state measurements, the fuel pressures were sensed by Autosyn type pressure transmitters, and the fuel flow was measured by rotameters.

All transient measurements were recorded on sensitized paper in a galvanometric oscilloscope. The galvanometer elements with natural frequencies from 200 to 500 cycles per second, depending on the amount of filtering desired, were used.

#### Control Computer

For the controls investigation, the necessary computation was performed by an electronic differential analyzer which comprises racks 4 to 6 of the equipment shown in figure 6. The computer performs the required operations through the use of high-gain d-c operational amplifiers and associated plug-in input and feedback impedances. Nonlinear operations such as multiplication are performed by computer elements contained in rack 4. For operations of the control systems, the output of the control computer is fed into the fuel control chassis which is located in rack 3. The recording equipment is shown in rack 1.

#### TEST PROCEDURE AND RANGE OF VARIABLES

The test program on the ram-jet engine covered the following range of flight conditions: flight Mach number, 1.5 to 2.16; ambient static pressure, 730 to 358 pounds per square foot absolute; angle of attack, zero to  $10^{\circ}$ ; and nozzle-exit area, 69 to 55 percent of the combustion-chamber area.

#### ENGINE DYNAMICS

In the engine-dynamics phase of the test program, the engine was subjected to disturbances in fuel flow. The secondary fuel flow was subjected to step changes of varying magnitudes from a number of initial levels covering the engine operating range including both supercritical and subcritical operation. During all imposed transients, the relevant dependent and independent engine variables were recorded on the oscilloscope.

### CONTROL TESTS

The steady-state performance of the control systems investigated was obtained by setting the various control systems in operation and observing the performance of the engine-control combination over a range of simulated flight conditions.

The control systems tested comprised two different control categories, continuous and discontinuous. In the former, the magnitude of the corrective action taken by the control is a continuous function of the error or departure from the control point. When corrective action is taken by the discontinuous control, the magnitude of the corrective action is independent of the magnitude of the error. This type of control is often referred to as an "on-off" control.

For the investigation of the dynamics of the continuous-control systems, the controlled engine was subjected to fuel flow disturbances by adding a step function to the output of the control. The response of the engine-control combination to these disturbances was recorded on the oscillograph. These tests were repeated for different settings of the control parameters over the range of flight conditions.

For the discontinuous-control systems, disturbances were introduced by manually bringing the engine fuel flow to a level which was away from the control point and then setting the control in operation. The manner in which these control systems restored the engine to the desired control point was recorded.

### RESULTS AND DISCUSSION

#### ENGINE STEADY-STATE PERFORMANCE

As noted in reference 2, the problem of control of a supersonic ram-jet engine may be resolved into the determination of the method of manipulation of the engine input variable to attain satisfactory, or desired, diffuser performance because the operating condition of the diffuser determines the thrust output and efficiency of the engine.

The performance of the engine used in the investigation reported herein is shown in figure 7. This figure shows the variation of diffuser pressure ratio (i.e., the ratio of diffuser-exit total pressure to ambient static pressure) with engine total-temperature ratio at several simulated flight Mach numbers and angles of attack. The engine total-temperature ratio is, of course, a function of the fuel-air ratio and the combustion efficiency.

At zero angle of attack, the engine operated both in the supercritical and subcritical regions (i.e., with the normal shock inside or outside the diffuser, respectively) throughout the range of Mach numbers. At this angle of attack, strong diffuser buzz existed in the subcritical region at Mach numbers of 1.79 and higher. At Mach 1.5, the diffuser pressure pulsations observed were of a much smaller order of magnitude than those observed at the higher Mach numbers.

At Mach 1.5 and  $10^{\circ}$  angle of attack, subcritical operation was possible although accompanied by diffuser buzz. At Mach 1.79 and  $10^{\circ}$  angle of attack, the engine operated erratically when subcritical operation was attempted and the engine frequently blew out. At Mach 1.99 and  $10^{\circ}$  angle of attack, it was impossible to obtain subcritical operation.

The following list indicates the ambient static pressures and the total temperatures which existed in the wind-tunnel test section at different flight Mach numbers:

Free-stream Mach number, $M_{\infty}$	Ambient pressure, lb/sq ft abs	Temperature, °R
1.50	730	565
1.79	545	585
1.99	460	610
<sup>a</sup> 2.16	<sup>a</sup> 358	610

<sup>a</sup>Engine-inlet condition only, attained by inclined-plate technique.

#### ENGINE DYNAMICS

The dynamic response of pressures within the ram-jet engine to disturbances in fuel flow was found to consist of two predominant phenomena. The first is a dead time and can best be illustrated by figure 8(a), which shows a typical transient response to a fuel flow disturbance with the engine operating in the supercritical region. For this run, the engine was operating at Mach 1.8 and zero angle of attack at an initial diffuser pressure ratio of 4.41. The engine was subjected to a fuel flow disturbance sufficient to bring it to a final pressure ratio of 5.14. It can be seen that the input voltage to the fuel servo was changed in a stepwise manner; and the fuel flow, which is a function of the secondary pressure, started to increase after a dead time of about 0.013 second and reached its final value about 0.04 second later. Four engine pressures are shown on the oscillogram, and it is seen that these pressures do not start changing in response to the change in fuel flow until approximately 0.025 second after the fuel flow had begun to change.

From a preliminary examination of the data taken, it appears that the dead time in the response of pressure to fuel flow varies from approximately 0.02 to 0.05 second over the range of engine and flight conditions investigated.

The second characteristic of the response of the engine pressures to fuel flow is a lead-lag characteristic, that is, a response which might be characterized by a transfer function of the type

$$G(s) = \frac{1 + \sigma \tau s}{1 + \tau s}$$

3409

This response characteristic is evident in figure 8(b), which is a typical transient record for supercritical engine operation at Mach 1.8 and zero angle of attack. The chart speed for this record is much less than that shown in figure 8(a) and brings out the lead-lag character of the response. The diffuser-exit pressures appear to respond directly proportional to fuel flow at first and then, after fuel flow reaches its final value, they approach the final steady-state value in an exponential manner. The dead time in the response is also evident in this record. Preliminary examination of the data shows that the rise ratio (i.e., the ratio of the initial jump to the total change in the variable) varied from 0.5 to 1.0 over the range of test conditions and that the time constant, which may be used to characterize the approximately exponential part of the response, varied from approximately 0.1 to 0.4 second over this same range.

#### CONTROLS INVESTIGATIONS

Because of the number of systems investigated, the description of the control systems and the characteristics observed will be discussed individually in the following sections.

##### Shock-Positioning Controls

Engine performance is directly related to the position of the normal-shock wave within the diffuser. Hence, normal-shock position can be employed as a control variable for the ram-jet engine. A series of such control systems was investigated during the test program.

The operating principles are given schematically in figure 9. These systems employed the pressure rise across a normal-shock wave to determine when the shock passed a given position.

The first system was designed to position the shock 15 inches downstream of the cowl lip (station d) and is sketched in figure 9(a). This system is designated the  $\Delta p_1$  control. A static pressure is sensed at

station d and a reference static pressure is sensed at a tap located at the cowl lip (station b, fig. 1(b)). The difference between these pressures is the control signal. If the fuel flow is too low, the normal shock is located downstream of both pressure taps. Because the area at station d is greater than that at station b and the flow is supersonic, the pressure at station d is less than the pressure at station b and the control calls for an increase in fuel flow. When the shock wave is between the two pressure taps, as in figure 9(a), the pressure at station d is much greater than the reference pressure, which causes the control to call for a decrease in fuel flow. If the normal shock is expelled, the pressure at station d is still greater than the reference pressure, because under these circumstances the flow within the diffuser is all subsonic and the greater area of station d results in a pressure higher than the reference pressure. This difference can be quite small, but still sufficiently large that proper control action can be taken.

OK-2  
6072

The second shock-positioning control system was designed to position the normal shock at a position 6 inches from the cowl lip (station c, fig. 1(b)) and is designated the  $\Delta p_{II}$  control. Station c has a flow area only slightly larger than that of the diffuser throat. The reference pressure tap was located at station a, which is on the diffuser cone surface 1 inch from the spike tip. This reference pressure location was chosen because it is sufficiently forward that, in the flight speed range considered, the engine temperature ratio available cannot force the normal shock to this point. When the normal shock is behind the desired location, the control pressure is approximately equal to the reference pressure; and when the shock is forward of the desired location, the control pressure is greater than the reference pressure (fig. 9(b)).

The third control system (fig. 9(c)) was designed to position the normal shock at the cowl lip and is designated the  $\Delta p_{III}$  control. The control pressure was sensed on the surface of the centerbody at station b. The reference pressure employed in this system was the same as that used for the  $\Delta p_{II}$  control.

The variation of the difference between the control pressure and the reference pressure is plotted as a function of fuel flow in figure 10 for all three shock-positioning controls. The term "adjusted" is applied to the coordinate definitions to account for the fact that all values were corrected to a set of standard pressures and temperatures in the test section of the wind tunnel, these variables being subject to the effects of the day-to-day variations in ambient atmospheric conditions at the laboratory. No individual data points are shown on these figures because the curves were obtained by graphical subtractions of appropriate pressure - fuel flow curves.

The pressure difference - fuel flow relation has a finite slope as the normal-shock wave passes the control point. This is the result of

the fact that at the stations used for control purposes the interaction of the shock wave and the boundary layer along the centerbody of the engine produces a gradual axial pressure profile across the shock zone rather than a discontinuity in pressure.

#### Continuous-Shock-Positioning Controls

The block diagram of the continuous-shock-positioning controls is shown in figure 11(a). In this system the controlled variable, the differential pressure, is sensed by a pressure transducer of the same type used in the engine-dynamics tests. The output signal of the transducer is amplified by a carrier amplifier which contains a biasing network that is used to set the desired value of the differential pressure, that is, the reference input to the control. The output of this amplifier is thus the error signal which is fed into the control computer that was set up in the electronic analog computer. The computer was wired as shown in figure 11(b) to yield proportional-plus-integral control action. The output of the computer is sent into the fuel servo system, which changes the fuel flow to the engine such that the set differential pressure is achieved.

The values of differential pressure set for the different controls are shown in figure 10. For the tests of engine-control dynamics, the disturbances were introduced by adding a step-function voltage of appropriate magnitude and sign to the summing network of the control computer (i.e., point  $\delta$  in fig. 11(b)).

Steady-state performance. - The steady-state performance of the continuous-shock-positioning control systems is shown in figure 12 superimposed on the engine map. The  $\Delta p_I$  control, which positioned the shock 15 inches downstream of the cowl lip, set a highly supercritical operating condition in the engine as indicated by the circular symbols. The  $\Delta p_{II}$  control system maintained the shock 6 inches downstream of the cowl lip, and the operating line which it set was quite close to peak engine performance. At Mach 1.5 it was necessary to rebias the control system because the set pressure differential of +560 pounds per square foot precluded satisfactory operation at this flight speed. The rebiased operating point is shown by the solid square symbol. The  $\Delta p_{III}$  control, designed to keep the normal shock at the cowl lip, provided the operating line shown by the diamond-shaped symbols. The engine operated slightly subcritical at Mach 1.99, but was at or near critical at other Mach numbers. Here again it was necessary to rebias the control system for operation at Mach 1.5 because the original choice of a bias of +600 pounds per square foot did not permit operation at this flight condition. It is apparent from the curves of figures 10(b) and (c) that a single judicious choice of the biasing point would have permitted satisfactory operation of both of the latter two control systems over the entire range

3409

of test conditions without the necessity of rebiasing the controls. This, of course, requires accurate knowledge of the engine calibration prior to setting up the control system.

Dynamic performance. - The dynamic-response characteristics of the continuous-shock-positioning control systems are shown in figures 13 and 15, wherein are plotted the variation of the response time of the controlled engine to disturbances in fuel flow as functions of loop gain, reciprocal integrator time constant, and disturbance sign. For the continuous controls, the response time is defined as the time required to reduce the error signal 63 percent. The loop gain is defined as the product of all the gains around the loop and the coefficient of the proportional-plus-integral control computer function  $K$ .

The response characteristics of the continuous  $\Delta p_I$  control are shown in figure 13 for a disturbance magnitude of 556 pounds per hour of fuel flow. The engine was operating at Mach 2.0 at zero angle of attack during these tests. It is seen that the response time decreased with decreasing integrator time constant and with increasing loop gain. For all the data shown in this figure, the system was stable and there was no sustained oscillation.

A typical transient response for the continuous  $\Delta p_I$  control system is shown in figure 14. This figure shows the response of the engine and control combination to a disturbance in fuel flow of +556 pounds per hour with the engine operating at Mach 2.0 and zero angle of attack. The control settings were: loop gain, 0.204; integrator time constant, 0.05 second. After the dead time in the response of the control pressure, the control acts to decrease the fuel flow to the engine, and the engine is returned to the set point in an almost exponential manner with but a slight undershoot. The response time for this particular transient is 0.18 second, which is represented by the solid data point of figure 13(a).

The response characteristics of the continuous  $\Delta p_{III}$  control are shown in figure 15. This control exhibited a variation of response time with control parameters similar to that observed for the  $\Delta p_I$  control.

A transient typical of those obtained for the continuous  $\Delta p_{III}$  control is shown in figure 16 for engine operation at Mach number 2.0 at zero angle of attack. The disturbance magnitude was +278 pounds per hour. Control settings were: loop gain, 3.04; integrator time constant, 0.02 second. The over-all dead time in the engine-control system is very evident in this record, with corrective action by the control being initiated about 0.035 second after the initiation of the transient in fuel flow. The response time for this transient is 0.13 second, which is represented by the solid data point of figure 15(a).

~~CONFIDENTIAL~~

Data covering a sufficiently wide range of control parameters are not available for the  $\Delta p_{II}$  control; however, the data that are available indicated response times of the same order of magnitude as those observed for the  $\Delta p_{III}$  control.

A typical transient response for the  $\Delta p_{II}$  continuous-shock-positioning control is shown in figure 17. For this run the engine was operating at Mach 2.0 at zero angle of attack and was subjected to a disturbance in fuel flow of +556 pounds per hour. The control settings were: loop gain, 2.32; integrator time constant, 0.033 second. The transient in fuel flow drove the engine into subcritical operation as can be seen from the oscillations in the diffuser-exit total-pressure and  $\Delta p_{III}$  traces. The control acted to reduce the fuel flow to the engine, and the resulting response time for this transient was 0.15 second.

All the continuous-shock-positioning controls exhibited the characteristic that the response time was different for positive and negative disturbances in fuel flow. This is partially the result of the choice of bias point in the control setting, which leads to saturation of the error signal sooner in one direction than the other, and can be inferred from the control variable curves of figure 10. The saturation of the error signal also leads to different response times for different magnitudes of disturbances.

#### Discontinuous-Shock-Positioning Controls

A block diagram of the shock-positioning control with discontinuous control action is shown in figure 18. Instead of a continuous error signal actuating the fuel servo, this type of control action uses an actuating signal of fixed magnitude generated by a differential-pressure switch sensing the difference in pressure between that at the control point and that at the reference pressure tap. The pressure switch used is shown schematically in figure 18(b). The internal volume of this switch is approximately 2 cubic centimeters. The switch has a rubber diaphragm secured between two electric contact points. Depending upon the magnitude of the pressure differential, the switch either closes one of the two contacts or neither contact is closed. The switch thus contains a pressure dead band. The closing of one or the other of the two contacts connects a control circuit to either a positive or negative fixed voltage source. The control circuit is an RC network energized by the input voltage from the switch. The voltage across the capacitor is amplified by a d-c amplifier, and the amplifier output is fed into the fuel servo input thus providing a fixed rate of change of fuel flow in response to the error signal. The characteristic time of the RC circuit was adjustable, permitting changes in the rate of change of fuel flow set by the control computer. The settings of the pressure switches used for the two discontinuous-shock-positioning controls tested are indicated in figures 10(a) and (c).

409

**3049**  
Steady-state performance. - The operating lines obtained from the discontinuous-shock-positioning control systems are shown in figure 19. Only  $\Delta p_I$  and  $\Delta p_{III}$  controls were investigated by this control technique. For the former, the operating lines are very similar to those obtained with the continuous-acting  $\Delta p_I$  control. The control designed to maintain the shock at the cowl lip ( $\Delta p_{III}$ ) operated from Mach 1.79 to 2.16, setting peak performance up to Mach 1.9 and then deviating to subcritical operation at Mach 1.99. Operation at Mach 1.5 was not possible with this system because of the setting of the pressure switch.

Dynamic performance. - The response characteristics of the discontinuous-shock-positioning controls are shown in figure 20, where the response time is plotted as a function of the rate of change of fuel flow. In general, the discontinuous controls investigated oscillated in steady state; therefore, for these control systems the response time has been defined as the time required for the controlled variable to first cross the set operating point during a transient. Because of the fixed rate of change of fuel flow set by the control system, the response time should vary approximately hyperbolically with the set rate of change of fuel flow for a fixed-disturbance amplitude. This characteristic is indicated on figure 20 by the dashed curves, which are plotted for disturbances in fuel flow of 1000 and 2000 pounds per hour. The data points shown are those obtained by displacing the engine from the operating point manually and then activating the control system. The amount the fuel flow was displaced is indicated for each data point. Response times were approximately the same for both positive and negative fuel flow displacements because of the constant rate of change of fuel flow set by the control system.

The amplitude of steady-state oscillation resulting from the discontinuous control action is shown in figures 21(a) and (b) for the  $\Delta p_I$  and  $\Delta p_{III}$  controls, respectively, as a function of the set rate of change of fuel flow. The control systems oscillated in steady state for all but the lowest set rates of change of fuel flow, and the observed oscillation was slightly greater for a given rate of change of fuel flow for the  $\Delta p_{III}$  control than for the  $\Delta p_I$  control. The oscillation amplitude increased linearly with increasing rate of change of fuel flow as was expected. The frequency of the oscillations in all cases was approximately 4.5 cycles per second. Because of the relations between response time, oscillation amplitude, and the set rate of change of fuel flow, it is apparent that the shorter the response time required for a given application the larger will be the steady-state oscillation.

In figure 22 is shown the response of the discontinuous  $\Delta p_I$  system after it had been activated with the engine operating at a fuel flow of 1600 pounds per hour above that which existed with the normal shock properly positioned. This high fuel flow placed the engine well within

the diffuser buzz region at Mach 2.0 and zero angle of attack as evidenced by the pulsations in the diffuser-exit pressure. The set rate of change of fuel flow for this transient was 7150 pounds per hour per second, and the almost linear change of fuel flow resulting yields a response time of 0.29 second with a residual steady-state oscillation of 755 pounds per hour of fuel flow at approximately 4.5 cycles per second. This corresponds to the solid circular data point of figure 20.

A typical transient history for the discontinuous  $\Delta p_{III}$  shock-positioning control is shown in figure 23. In this transient the control was put in operation after the engine had been manually placed at an operating condition where the fuel flow was 1370 pounds per hour below that required for the desired operating condition at Mach number 2.0 and zero angle of attack. The response time for this transient is 0.26 second, and the residual steady oscillation was equivalent to 805 pounds per hour of fuel flow for the set rate of change of fuel flow of 7150 pounds per hour per second. This transient corresponds to the solid square data point of figure 20.

3409

#### Flight Mach Number Control Based On Discontinuous- Shock-Positioning Principles

A control system designed to regulate the flight Mach number of a ram-jet vehicle and employing the principles of discontinuous shock positioning was investigated during the test program. The system is a cascade of two shock-positioning controls so arranged that the engine will produce high thrust at Mach numbers below the design Mach number of the inlet and will produce a reduced thrust at flight Mach numbers above the design value.

The principle of operation of this control system is shown in figure 24. The difference in the pitot pressure measured at the cowl lip  $P_l$  and the pitot pressure measured at the tip of the inlet cone  $P_0'$  is sensed by a differential-pressure switch. This pressure is used in a shock-positioning loop designed to position the normal shock such that the slip line generated at the intersection of the oblique and normal shocks intercepts the tube measuring  $P_l$ . This is designated the primary loop or system.

At flight Mach numbers below design, the conditions shown in figure 24(a) prevail. If the fuel flow is too low, the normal shock will be close to the inlet and the slip line will pass outside of the cowl. Under these conditions the pitot pressure measured at the cowl will be greater than that measured at the tip of the spike, and the control acts to increase the fuel flow. This forces the normal shock forward until the slip line falls within the cowl. The pressure at the cowl is then

approximately equal to that at the tip of the spike and this causes the pressure switch in the primary loop to set a secondary loop in operation. This secondary loop is the  $\Delta p_I$  control system which acts to reduce the fuel flow, because the shock is too far forward for the  $\Delta p_I$  system. The combined control action of these two systems results in subcritical operation for flight Mach numbers below inlet design Mach number, which yields essentially maximum thrust. As the flight Mach number increases, the oblique-shock angle decreases, the normal shock approaches closer to the cowl lip, and the engine approaches critical operation at inlet design Mach number (fig. 24(b)). As flight Mach number increases further, the oblique shock falls within the cowl lip (fig. 24(c)), which results in equal pressures at the cowl lip and at the tip of the cone. Under these conditions the primary switch always activates the secondary system and the engine operates on the  $\Delta p_I$  control yielding a low thrust level.

For application to a missile speed control system, the engine would have to be designed so that with critical engine operation there would be a thrust margin at the inlet design Mach number, and the reduced thrust provided by the secondary control system would have to be below that which would sustain flight at constant velocity. With this arrangement the over-all control system would act to set the missile flight speed at the engine-inlet design speed and the missile velocity would tend to oscillate about this point.

A block diagram of this control system is shown in figure 25. The two differential pressures are sensed by pressure switches; and depending upon flight Mach number and engine conditions, the appropriate shock-positioning system functions and sends a signal to a control circuit which provides a constant rate of change of fuel flow to the engine, increasing or decreasing the fuel flow depending upon the sign of the error signal. The interconnections of the two pressure switches are shown in figure 25(b). The primary switch is so arranged that, when the differential pressure is approximately zero, it activates the secondary switch which is connected as for the  $\Delta p_I$  shock-positioning control.

The differential pressure sensed by the primary pressure switch is shown as a function of fuel flow for several Mach numbers in figure 26. The primary pressure switch was set so that for differential pressures greater than +35 pounds per square foot it would close the circuit, calling for an increase in fuel flow; and for differential pressures less than +25 pounds per square foot the primary switch would activate the secondary pressure switch and, hence, the  $\Delta p_I$  control. At Mach 2.16, which is shown in figure 26(a), it is seen that the secondary switch is always activated. At Mach 1.8, the secondary switch could be activated when the fuel flow was between 3600 and 3900 pounds per hour. This is, in effect, an additional dead band in the control and is largely of aerodynamic origin, caused by the thickness of the slip "line." At

~~CONFIDENTIAL~~

Mach 1.5, the intersection of the oblique and the expelled normal shock is further forward, which results in a still thicker slip "line" at the cowl-lip measuring station. At this flight condition the over-all dead band is equivalent to approximately 500 pounds per hour of fuel flow.

The engine operating line obtained under action of this control system is superimposed on the engine performance map in figure 27. For flight Mach numbers from 1.5 to approximately 1.9, the control system set subcritical operating conditions; the effect of the aerodynamic dead band is indicated by the shaded area. At Mach numbers above 1.9, the secondary system was in operation and an operating line similar to that obtained from the  $\Delta p_I$  shock-positioning control resulted.

The dynamic performance characteristics of this control system are similar to those resulting from the other discontinuous-shock-positioning control systems. A data point for this control system operating at Mach 1.5 is shown on figure 20 and is seen to agree with similar data for the other discontinuous-shock-positioning controls. The effect of the set rate of change of fuel flow on steady-state oscillation amplitude for this control system is shown in figure 28. The oscillation amplitude again increases with the rate of change of fuel flow. The effect of the aerodynamic dead band is evident in the figure. Because of the dead band, no steady-state oscillations were observed below a set rate of change of fuel flow of 7150 pounds per hour per second at Mach 1.8 and 5200 pounds per hour per second at Mach 1.5. In the regions where no oscillations existed, the fuel flow and hence the engine operating point could drift within the dead band. This is observed in figure 29, which shows a typical transient response for this control system operating at Mach 1.5 and zero angle of attack. The engine had been displaced from the operating point by reducing the fuel flow by 1990 pounds per hour. The set rate of change of fuel flow was 2450 pounds per hour per second, which is within the region of operation where the aerodynamic dead band acts to prevent sustained steady-state oscillation. The system crossed the final values in 0.775 second, and the fuel flow drifted about in the dead band and finally appeared to settle out; this is represented by the solid diamond data point of figure 20.

#### Direct Control of Diffuser Pressure

As noted in reference 2, the relation that exists between the pressure at the exit of the diffuser and the thrust of a ram-jet engine can be used in an engine control system. The variation of diffuser pressure ratio with fuel flow at several Mach numbers is shown in figure 30 for the engine used in this investigation. This relation can be used to obtain a given diffuser pressure ratio via closed-loop control provided operation in the subcritical region at pressure ratios below the set value is prevented.

~~CONFIDENTIAL~~

3409

The reference input to the control system is the set value of diffuser pressure ratio, and some means must be provided to obtain a desired schedule of this set value as a function of flight Mach number, altitude, and so forth. One such system was employed during the test program reported herein. This system used what might be termed an aerodynamic computation of the desired diffuser pressure ratio as a function of flight Mach number and inherently provided the required compensation for the effects of altitude pressure.

A small replica of the inlet spike was constructed with a total-pressure tube located above the cone surface so that, in the Mach number range of the tests, the tube was always behind the conical shock wave. Thus, the pressure measured by this tube is that behind an oblique- and a normal-shock wave and represents the maximum pressure capability of the diffuser. The variation of this total pressure  $P_{ac}$  with Mach number and angle of attack is shown in figure 31. Also shown on this figure is the variation of the peak diffuser pressure ratio of the engine at several angles of attack. For angles of attack up to  $5^\circ$ , there is an almost constant ratio between  $P_{ac}$  and  $P_{x,max}$  in this flight Mach number region. As a simple test for this method of computation, a fixed percentage of the total pressure measured above the auxiliary cone was used as the input signal for the control system. During the test program, two such schedules were used, 90 percent and 85 percent of  $P_{ac}$ . These are shown on figure 31 as the dashed lines.

The block diagram of the system tested is shown in figure 32. The system comprises two loops, the first is the basic control loop and the second is a limiting loop to prevent engine operation in the region which would normally result in positive feedback in the basic loop.

In the basic control loop, the total pressure above the auxiliary cone is sensed by a pressure transducer and the output is amplified by a carrier amplifier set so that its output represents a fixed percentage of the measured pressure. The amplifier output is then the reference or set value of the diffuser pressure. The total pressure at station  $x$  is sensed by a pressure sensor in the engine and is suitably amplified by a carrier amplifier. This signal is then compared to the reference signal in an error detector and the difference between the two signals, or error, is transmitted to the proportional-plus-integral control computer set up on the analog computer. The output of the computer is fed into the fuel servo, which then acts to change the fuel flow in such a manner that the error is reduced to zero.

The limiting circuit operates in the following manner: The differential pressure corresponding to the  $\Delta p_{III}$  shock-positioning control signal is sensed and amplified by a carrier amplifier. This amplifier is so biased that in the event the normal shock passes the cowl lip

6043

CK-5

CONFIDENTIAL

during a transient a large negative signal is produced and the fuel flow is reduced. This circuit is operative only during such a transient and thus prevents positive feedback in the basic control system.

Steady-state performance. - The steady-state operating lines obtained during the tests of this control system are shown on figure 33. Two set pressure values are shown in this figure, 90 and 85 percent of  $P_{ac}$ . The 90-percent schedule was set up at Mach 1.5 and operated satisfactorily up to Mach 1.79. At Mach 1.99 this system failed to operate properly. It was found that this was the result of the fact that a single total-pressure tube was used to sense the pressure at station x. Up to Mach 1.8 this tube indicated a pressure very close to the average pressure at station x. At Mach numbers above 1.8, there is a shift in the pressure profile at station x, and the particular tube used no longer indicates a pressure close to the average value. Instead, it reaches a peak value well below the peak average pressure. Failure of the system at Mach 1.99 indicates that the peak value of pressure from the single tube was nearly equal to or possibly slightly less than 90 percent of  $P_{ac}$ . This indicates the necessity of using an averaging rake in the engine to sense the controlled pressure. Because it was inconvenient to do this during the test program, the schedule was changed so that it set 85 percent of  $P_{ac}$  as the desired pressure. The control then operated as expected in the Mach number range from 1.8 to 2.0.

6409

It should be noted that the schedule used is only one of many possible schedules and that any schedule may be used with this type of control as long as the schedule requirements are within the limits of engine operation.

Dynamic performance. - The dynamic-response characteristics of this control system are shown in figure 34 for operation at Mach 1.5 and zero angle of attack. The variation of response time with reciprocal integrator time constant and loop gain is shown for disturbances in fuel flow of  $\pm 556$  pounds per hour. The response time decreases with decreasing integrator time constant, reaching a value of approximately 0.06 second at an integrator time constant of 0.01 second with a loop gain of 0.39. With an integrator time constant of 0.05 second, the response time reaches approximately 0.05 second at a loop gain of 1.56. All the data shown in figure 34 represent system operation with no residual steady-state oscillation. For positive disturbances (increased fuel flow) the response time is larger than for negative disturbances.

A typical transient response of the engine-control system is shown in figure 35. The engine was operating at Mach 1.5 and zero angle of attack with the control on the 90-percent schedule. The system was disturbed from equilibrium by decreasing the fuel flow by 556 pounds per hour. The over-all system dead time can be seen in the servo input voltage trace, where the flat portion of the response indicates the time

necessary for the diffuser-exit pressure to change as a result of the fuel flow disturbance so that the control may begin to return the engine to the set operating point. For this transient response the control was set with an integrator time constant of 0.01 second and a loop gain of 0.39. This yielded a response time of 0.064 second with only a slight overshoot. This transient is represented by the solid data point of figure 34(a).

#### Peak-Holding Optimizer Control

The peak in the pressure ratio - fuel flow characteristics shown in figure 30 for the ram-jet engine used in this investigation makes possible the use of peak-holding optimizer control principles as indicated in references 2 and 7. The peak pressure ratio occurs at or very near the critical operating condition for the ram-jet engine and therefore provides a means of control that always produces maximum thrust most efficiently.

The optimalizing control used in this investigation employed a test-signal technique. Consider the effect of imposing a test signal in fuel flow on the ram-jet engine whose characteristics are shown in figure 30. Let the test signal be sinusoidal in nature and be represented by

$$\Delta W_f = A \sin \omega t$$

When the engine is operating in the supercritical region, the diffuser pressure will vary in response to the change in fuel flow in this manner:

$$\Delta P_x = B_{sup} \sin \omega t$$

When the engine is operating in the subcritical region, the pressure variation caused by the test signal would be given by

$$\Delta P_x = -B_{sub} \sin \omega t$$

Consider now the effect of multiplying the input and output signal under these two conditions of engine operation. For supercritical operation,

$$\Delta W_f \Delta P_x = AB_{sup} \sin^2 \omega t = \frac{AB_{sup}}{2} (1 - \cos 2\omega t)$$

and for subcritical operation,

$$\Delta W_f \Delta P_x = -AB_{sub} \sin^2 \omega t = -\frac{AB_{sub}}{2} (1 - \cos 2\omega t)$$

6042

CK-3 back

CONFIDENTIAL

NACA RM E54H10

If these product signals are suitably filtered, only the d-c component will remain and as a result the following is obtained: For supercritical operation the filtered signal would be  $AB_{sup}/2$  and for subcritical operation,  $-AB_{sub}/2$ . Because of the difference in sign, these signals can be used to actuate a fuel control which would act to hold peak pressure in the diffuser by increasing the mean fuel flow for supercritical operation and to decrease the mean fuel flow for subcritical operation.

This technique was applied during the test program on the ram-jet engine, and a block diagram of the system used is shown in figure 36. The test signal is applied simultaneously to two places, a multiplier in the analog computer and the fuel servo input, where it is added to the existing input voltage. The fuel flow then varies periodically about some average value, and this results in variations in the total pressure at station x. This total pressure is sensed by a pressure transducer, and the output of the sensor is amplified by a carrier amplifier. The amplifier output is passed through a band-pass filter to remove the d-c level in the signal and also to remove noise in the signal at frequencies above that of the test signal. The filter output is then fed into the multiplier, where it is multiplied by the test signal. The multiplier output is sent through a low-pass filter to remove the a-c (i.e.,  $\cos 2\omega t$ ) term, and the filter output is sent into the fuel servo system to vary the average fuel flow to the engine.

Steady-state performance. - The control system was tested on the ram-jet engine over the range of Mach numbers from 1.5 to 1.99. The operating line achieved is shown in figure 37, where it is superimposed on the engine operation map. The test-signal magnitude was equivalent to an amplitude of 131 pounds per hour in fuel flow and was applied at a frequency of 2.0 cycles per second. The control held the engine at or near peak pressure recovery from Mach 1.5 to 2.0, and the magnitude of the test signal was sufficiently small that it did not appreciably affect the steady-state performance of the engine.

Dynamic performance. - The dynamic performance of the optimalizer control is shown in figure 38 for the engine and control operating at Mach 1.6 and zero angle of attack. The figure shows the variation of response time with reciprocal integrator time constant for fuel disturbances of 556 pounds per hour. At constant control gain of 0.1, the response time is seen to decrease with decreasing integrator time constant, reaching a response time of approximately 0.4 second at an integrator time constant of 0.05 second. It can be seen that the response time is much smaller for negative disturbances than for positive disturbances in fuel flow. This is to be expected because, as seen in figure 30, the slope of the pressure ratio - fuel flow curve is steeper in the supercritical region than in the subcritical region and this leads to larger corrective signals for negative disturbances than those for positive disturbances in fuel flow. It should be noted that, despite the

almost zero slope of the pressure - fuel flow relation of the engine at Mach 1.5 in the subcritical region, the control functions properly although the response time is correspondingly large.

A typical transient response of the optimalizer control is shown in figure 39. For this transient the engine was operating at Mach 2.0 and zero angle of attack, and the system was subjected to a disturbance in fuel flow of -556 pounds per hour. The test signal is a sine wave. In steady state, the filtered pressure signal, which is one of the inputs to the multiplier, is seen to have the characteristic double frequency resulting from oscillation about a peak. This shifts to the test-signal frequency during the portion of the transient when the engine is operating entirely in the supercritical region and then reverts to the double frequency when it approaches the steady-state value. For this particular trace the integrator time constant was set at 0.05 second and the computer gain was 0.05, which yielded a response time of 1.1 seconds.

#### CONCLUDING REMARKS

The information contained herein, which was obtained from a supersonic wind-tunnel investigation of ram-jet engine controls and dynamics, is of a preliminary nature.

The three types of control systems investigated (shock positioning, direct control of diffuser pressure, and optimalizing) operated satisfactorily, and all offer practicable means of controlling ram-jet engine operation. All the systems responded satisfactorily to large disturbances, including disturbances that placed the engine well into the diffuser buzz region.

Of the control systems tested, the shock-positioning systems were the simplest to implement and were followed in order of complexity by the direct control of diffuser pressure and the optimalizer control.

The response of engine pressures to disturbances in fuel flow appears to be a combination of a dead-time- and a lead-lag-type response. The dead time varied from approximately 0.02 to 0.05 second, the rise ratio from 0.5 to 1.0, and the time constant of the exponential portion of the lead-lag from 0.1 to 0.4 second.

Lewis Flight Propulsion Laboratory  
National Advisory Committee for Aeronautics  
Cleveland, Ohio, August 17, 1954

## APPENDIX - SYMBOLS

The following symbols are used in this report:

A	test-signal amplitude for optimalizer control	3409
B	slope of diffuser-exit total pressure - fuel flow curve	
C	capacitance	
G	general function	
K	gain of proportional part of control	
M	Mach number	
P	total pressure	
p	static pressure	
R	resistance	
s	complex operator	
t	time	
V	voltage	
$V_i$	input voltage to fuel servo	
$V_f$	position feedback voltage of fuel valve	
$V_1$	pressure-sensor output voltage	
$V_2$	control feedback voltage	
$V_3$	control-computer output voltage	
$W_f$	fuel flow, lb/hr	
$\alpha$	angle of attack, deg	
$\Delta p_n$	fuel nozzle pressure drop	
$\Delta p_I$	$p_d - p_b$	

$\Delta p_{II}$   $p_c - p_a$

$\Delta p_{III}$   $p_b - p_a$

$\delta$  disturbance function

$\Lambda$  percentage of maximum potentiometer resistance in control computer circuit/100

$\sigma$  rise ratio

$\tau$  time constant

$\tau_r$  integrator time constant

$\omega$  angular frequency, radians/sec

Subscripts:

a 1 in. behind cone tip

ac auxiliary cone

b plane of cowl lip

c 6 in. inside cowl lip

d 15 in. inside cowl lip

e error

l cowl lip

max maximum

sub subcritical

sup supercritical

x diffuser exit

1 engine inlet

3 combustion-chamber inlet

4 nozzle inlet

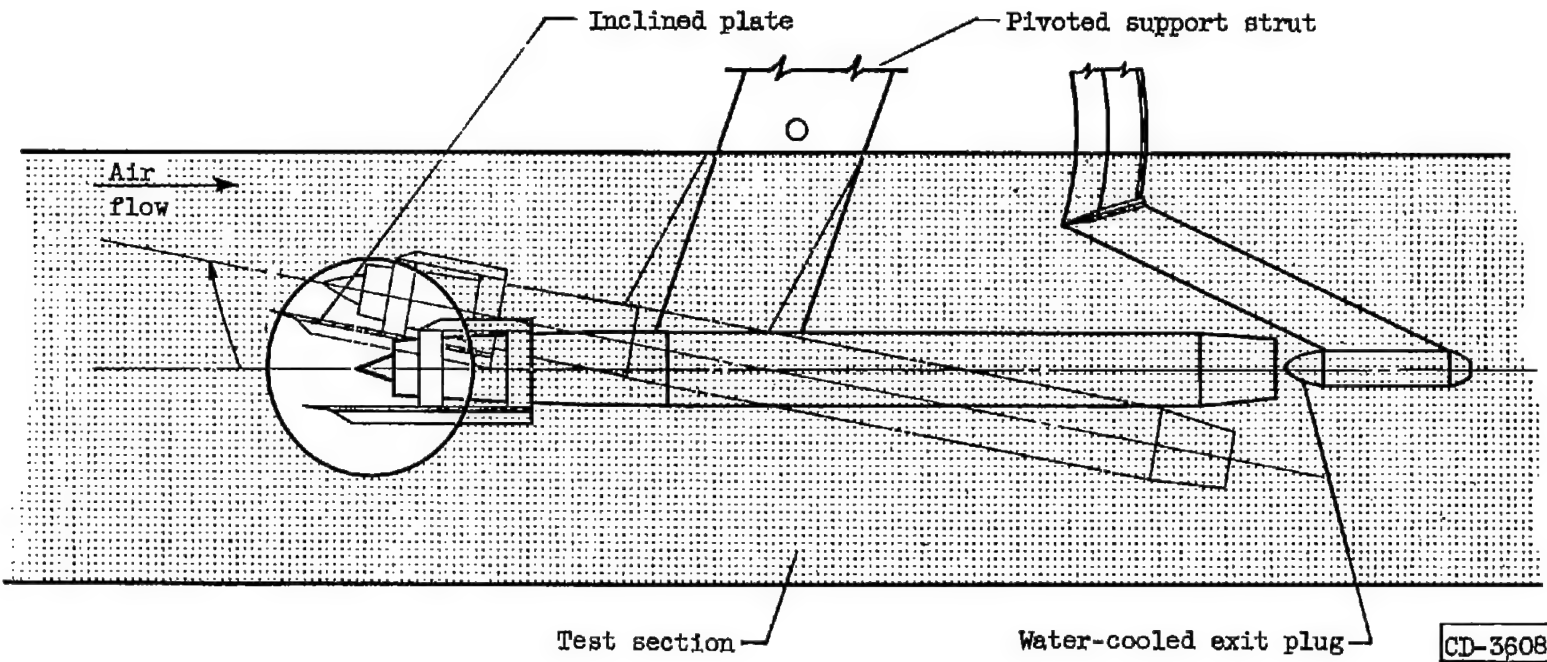
6 engine exit

Superscript:

pressure behind normal shock

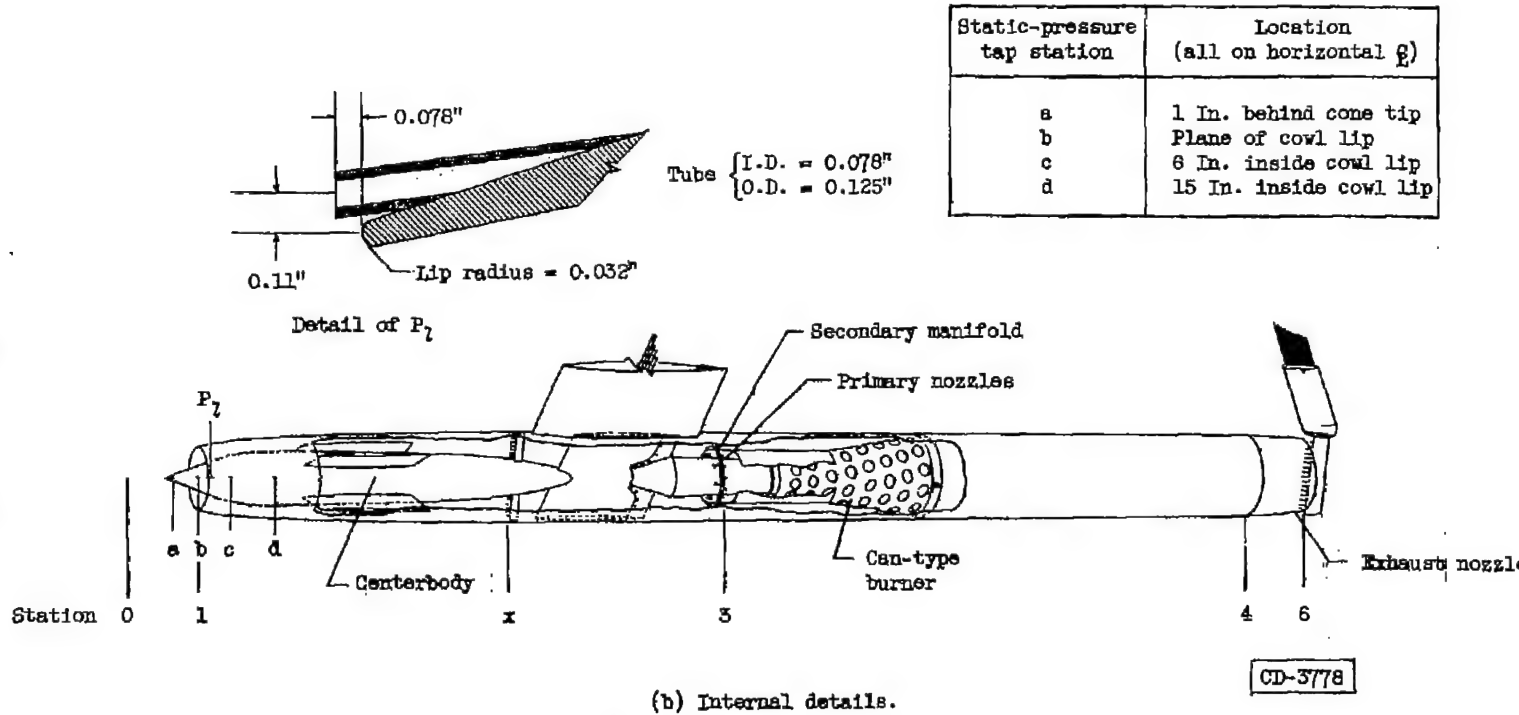
REFERENCES

1. Boksenbom, Aaron S., and Novik, David: Control Requirements and Control Parameters for a Ram Jet with Variable-Area Exhaust Nozzle. NACA RM E8H24, 1948.
2. Himmel, Seymour C.: Some Control Considerations for Ram-Jet Engines. NACA RM E52F10, 1952.
3. Hearth, Donald P., and Perchonok, Eugene: Performance of a 16-Inch Ram-Jet Engine with a Can-Type Combustor at Mach Numbers of 1.50 to 2.16. NACA RM E54G13, 1954.
4. Fox, Jerome L.: Supersonic Tunnel Investigation by Means of Inclined-Plate Technique to Determine Performance of Several Nose Inlets over Mach Number Range of 1.72 to 2.18. NACA RM E50K14, 1951.
5. Gold, Harold, Otto, Edward W., and Ransom, Victor L.: Dynamics of Mechanical Feedback-Type Hydraulic Servomotors Under Inertia Loads. NACA Rep. 1125, 1953. (Supersedes NACA TN 2767.)
6. Gold, Harold, and Otto, Edward W.: An Analytical and Experimental Study of the Transient Response of a Pressure-Regulating Relief Valve in a Hydraulic Circuit. NACA TN 3102, 1954.
7. Draper, C. S., and Li, Y. T.: Principles of Optimalizing Control Systems and Application to the Internal Combustion Engine. Aero. Eng. Dept., M.I.T., pub. by A.S.M.E., Sept. 1951.



(a) Installation in 8- by 6-foot supersonic wind tunnel.

Figure 1. - 16-Inch ram-jet engine.



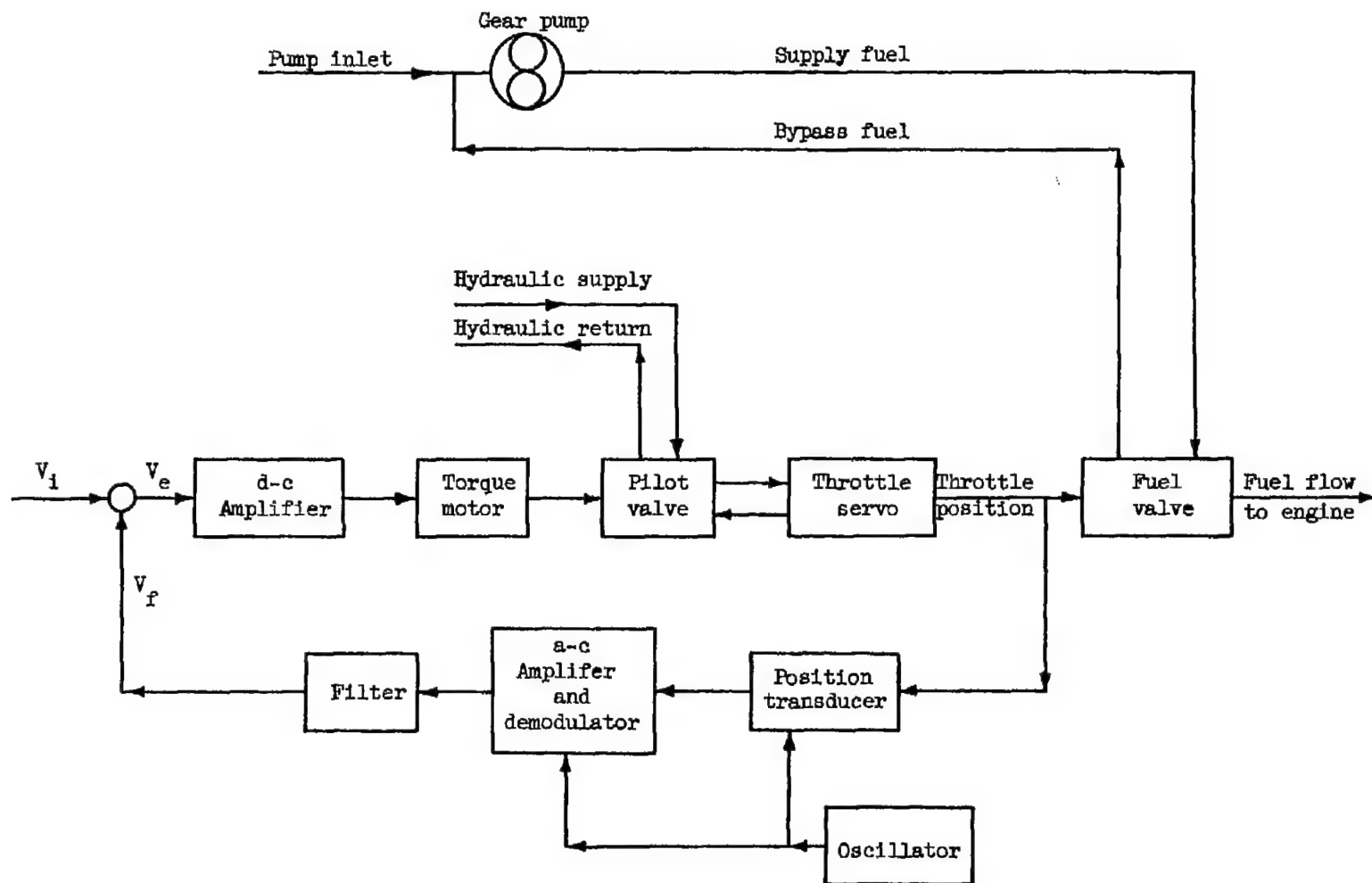


Figure 2. - Schematic diagram of fuel system.

CONFIDENTIAL

NACA RM 354HO

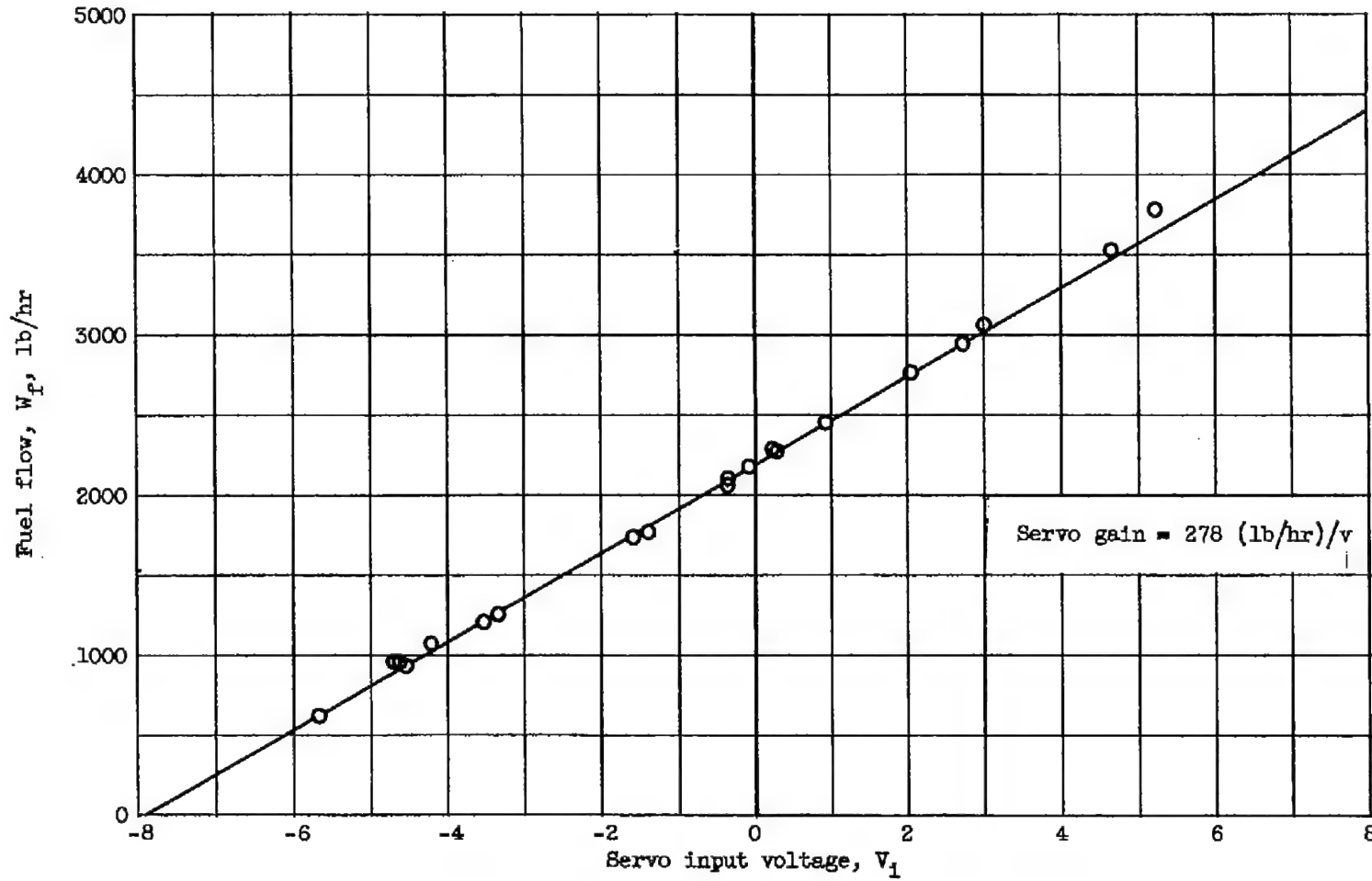
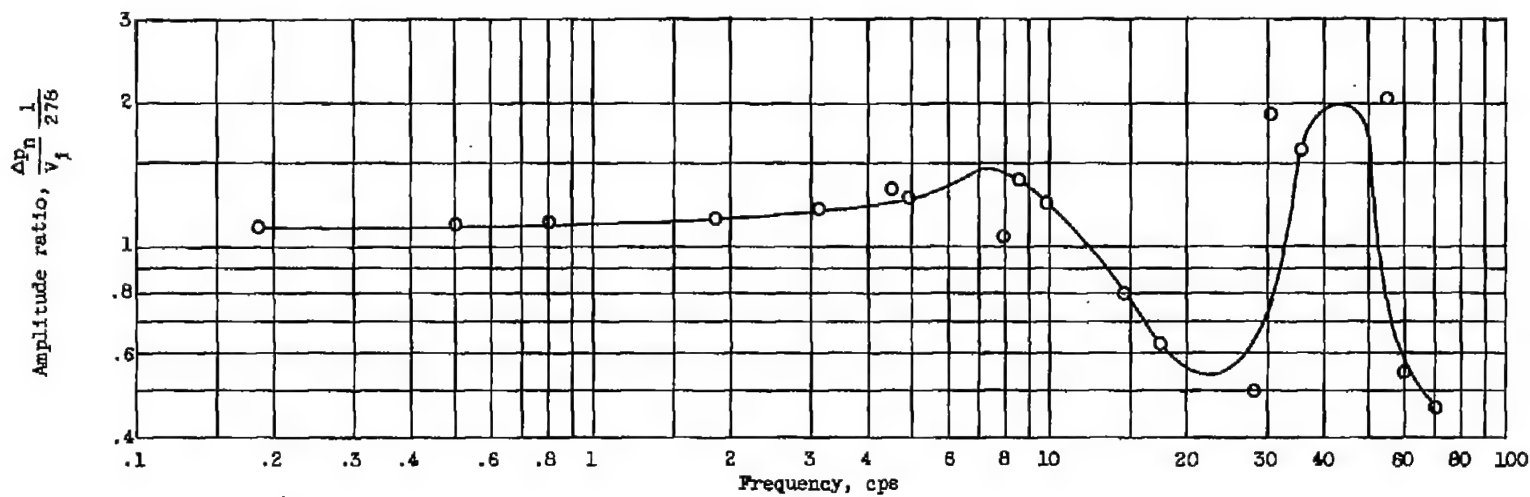
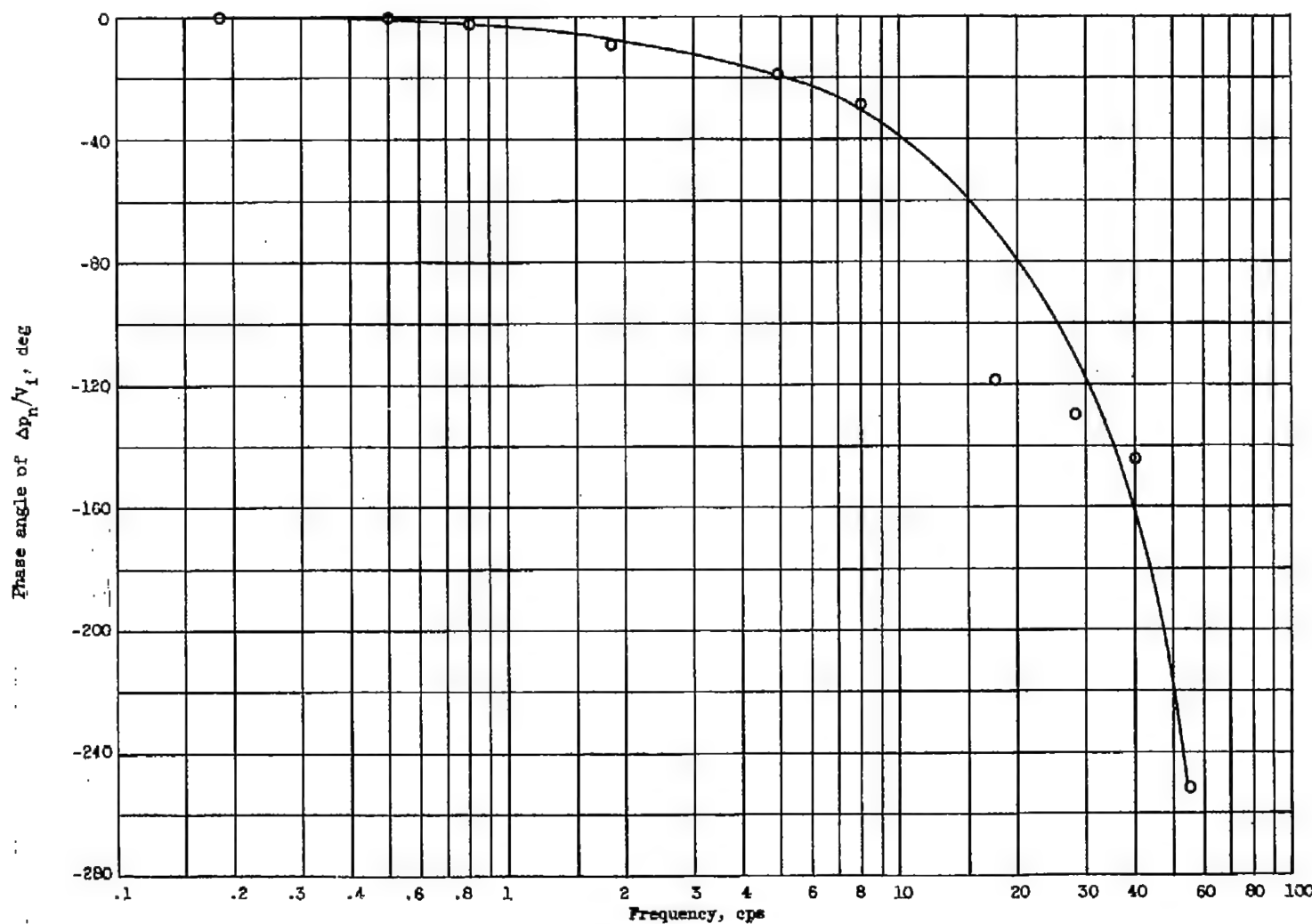


Figure 3. - Steady-state performance of fuel system.



(a) Amplitude ratio.

Figure 4. - Typical frequency response of fuel system.



(b) Phase shift.

Figure 4. - Concluded. Typical frequency response of fuel system.

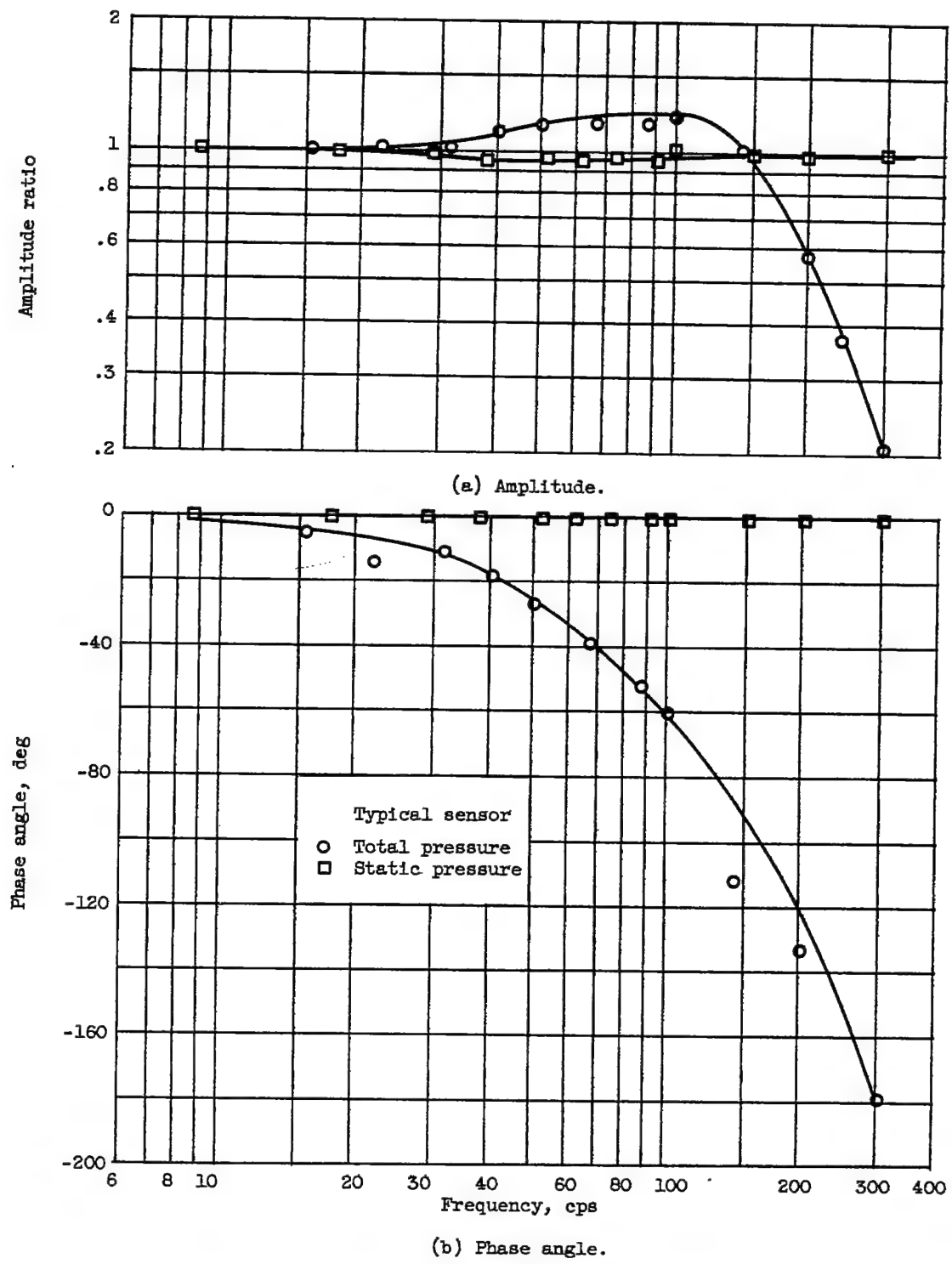


Figure 5. - Typical frequency response of pressure transducers.

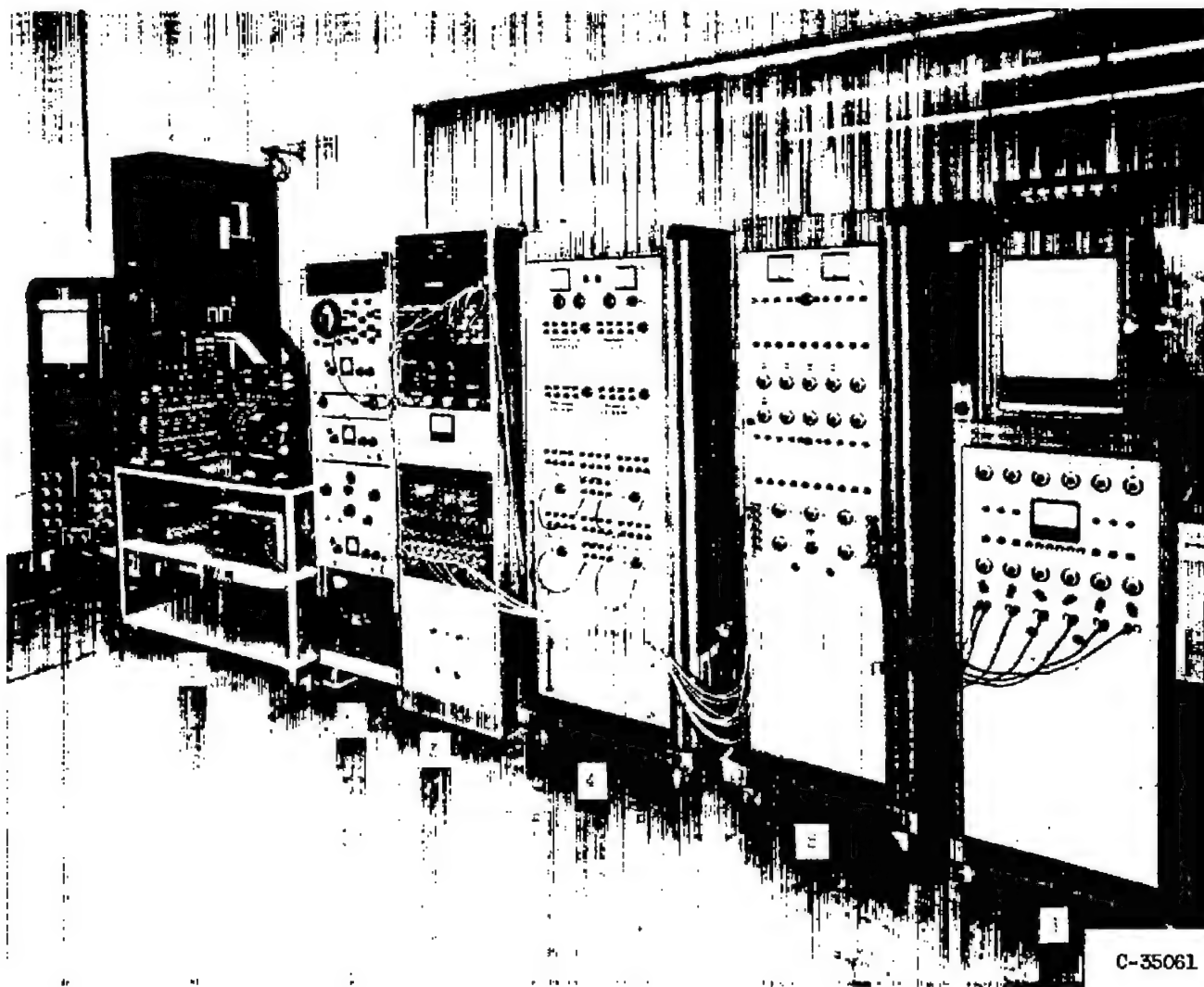
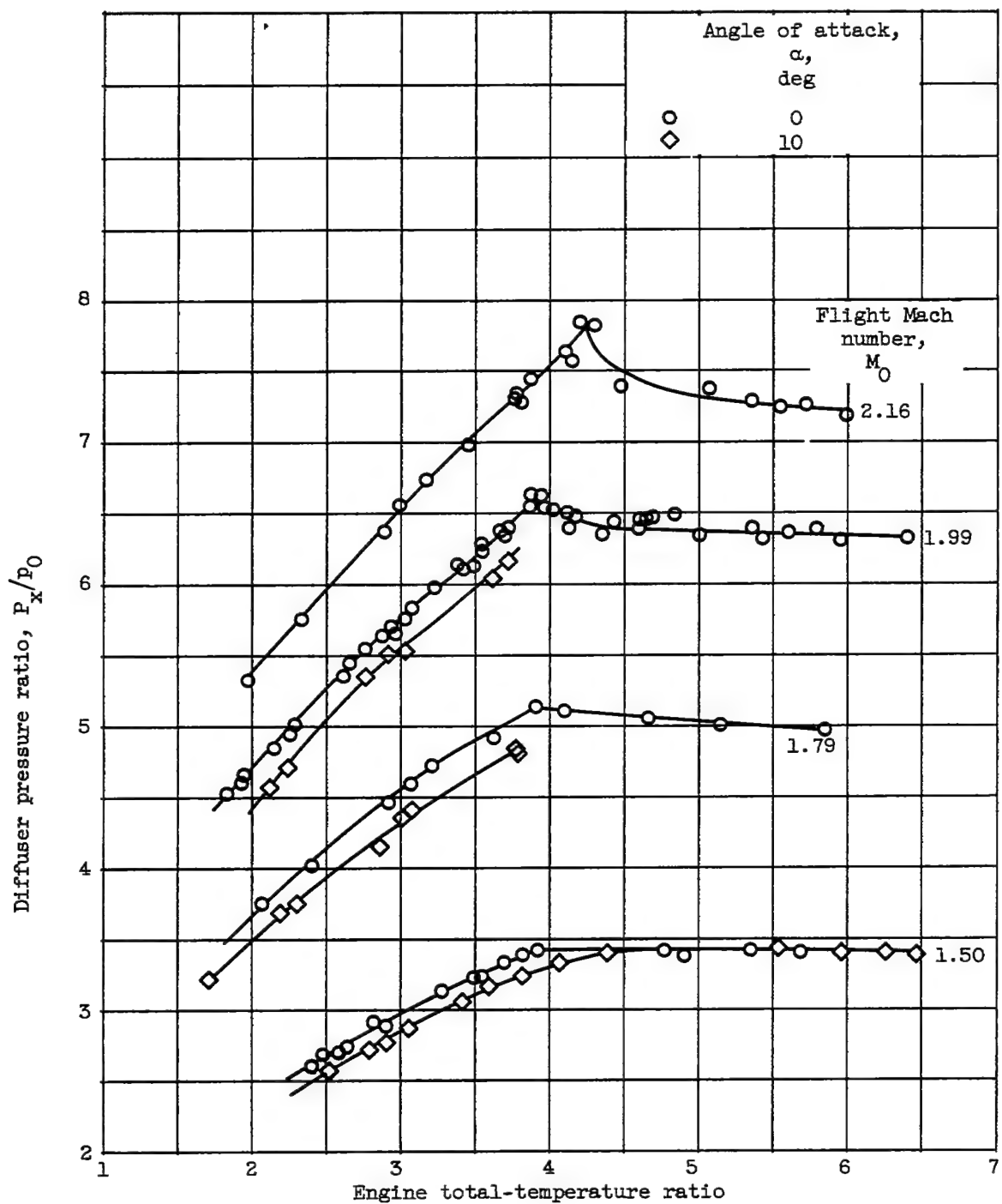
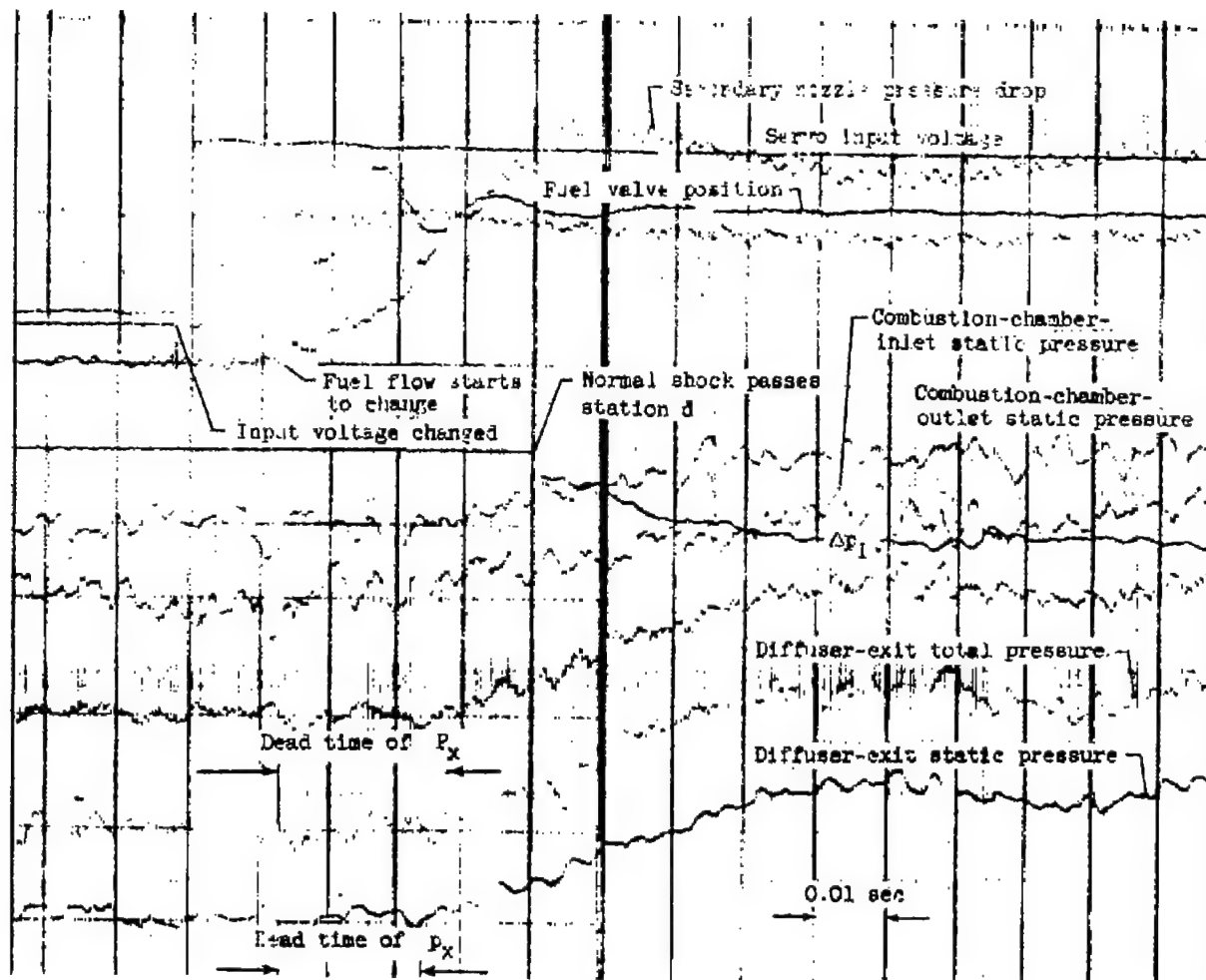


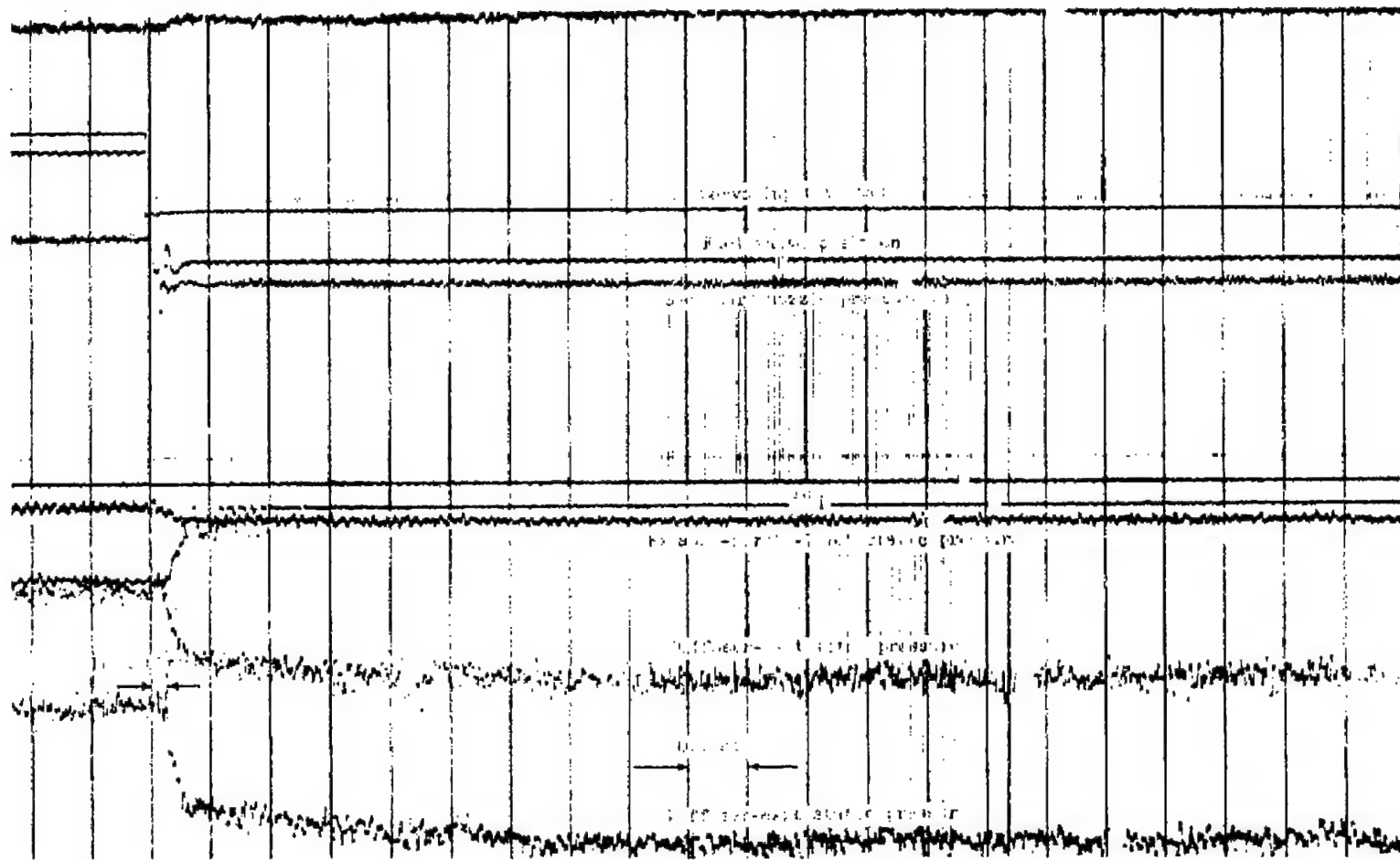
Figure 6. - Control computer and equipment.

Figure 7. - Engine performance. Exit area  $A_6$ , 0.960 square foot.



(a) High chart speed trace showing dead time. Initial diffuser pressure ratio, 4.41; final diffuser pressure ratio, 5.14.

Figure 8. - Engine response to step input in fuel flow. Flight Mach number  $M_0$ , 1.8; zero angle of attack.



(b) Low chart speed trace showing lead-lag characteristic. Initial diffuser pressure ratio, 4.93; final diffuser pressure ratio, 4.37.

Figure 8. - Concluded. Engine response to step input in fuel flow. Flight Mach number  $M_0$ , 1.8; zero angle of attack.

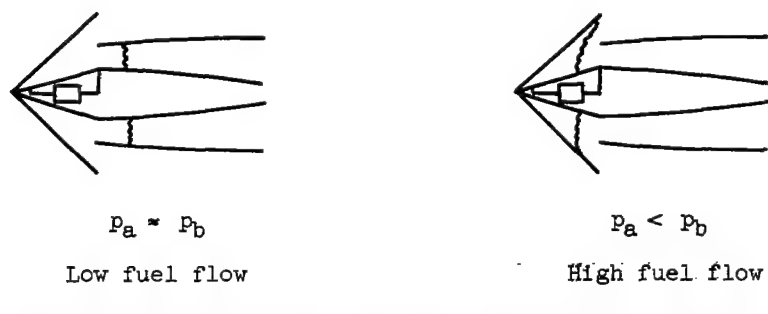
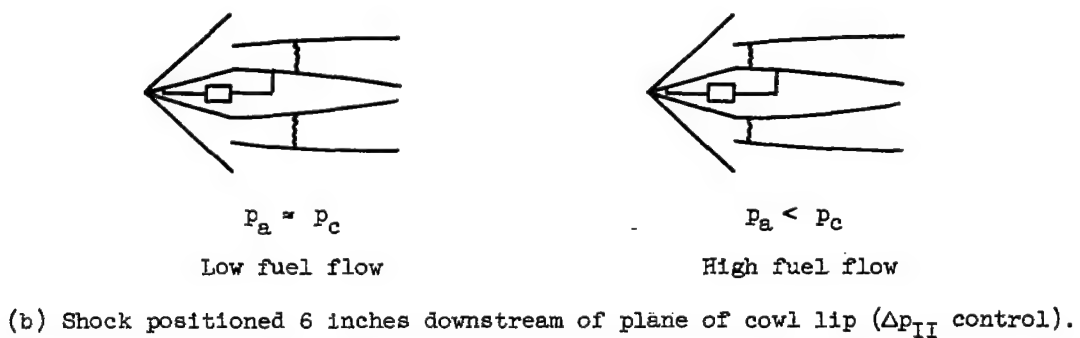
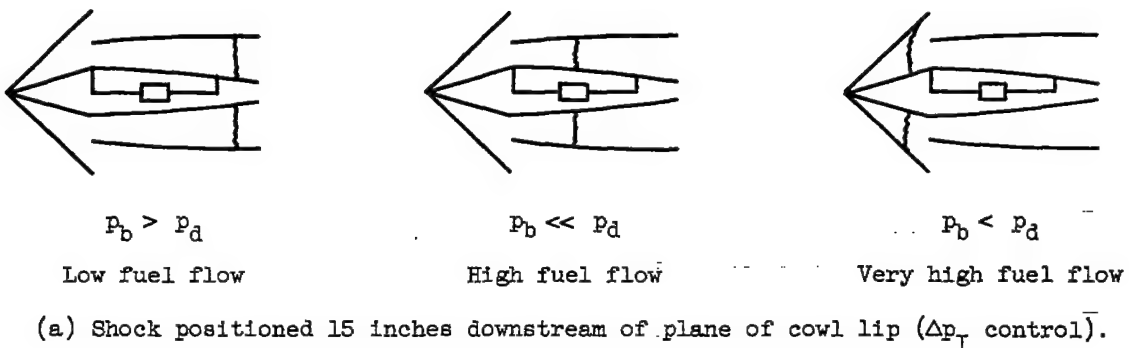


Figure 9. - Principles of operation of several shock-positioning controls.

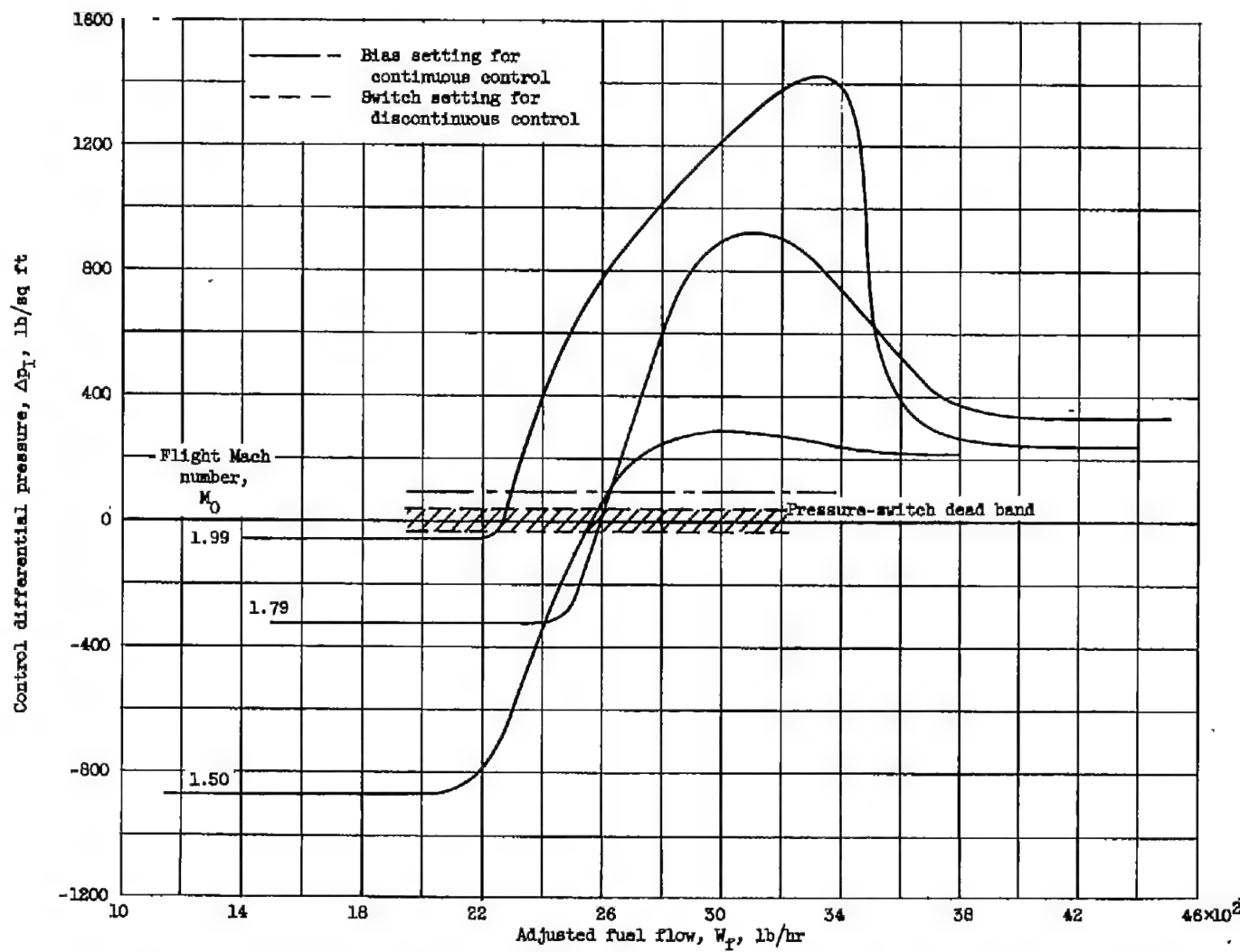
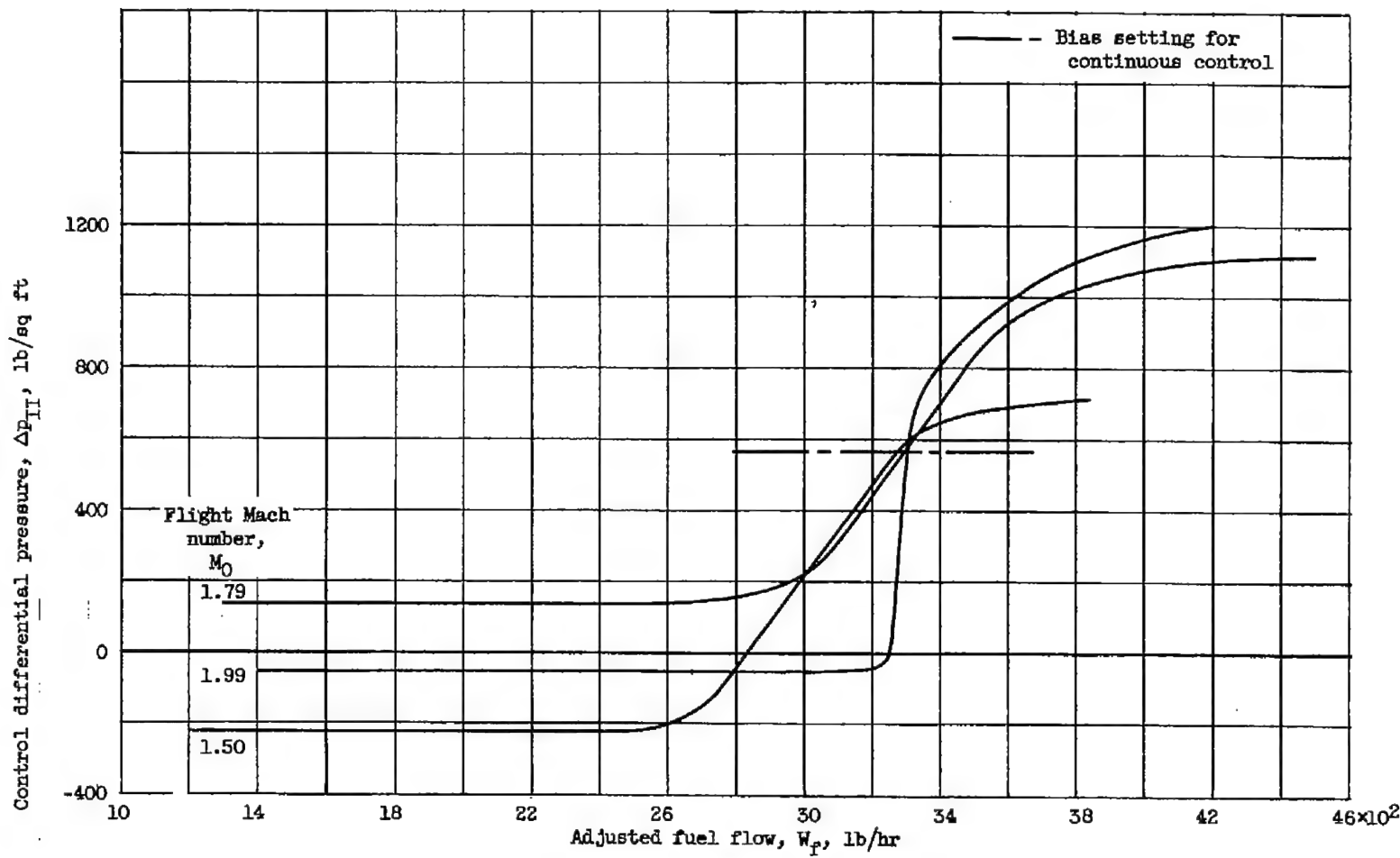
(a) Control,  $\Delta P_t$ .

Figure 10. - Variation of control pressure for shock-positioning controls with fuel flow at several flight Mach numbers.



(b) Control,  $\Delta p_{II}$ .

Figure 10. - Continued. Variation of control pressure for shock-positioning controls with fuel flow at several flight Mach numbers.

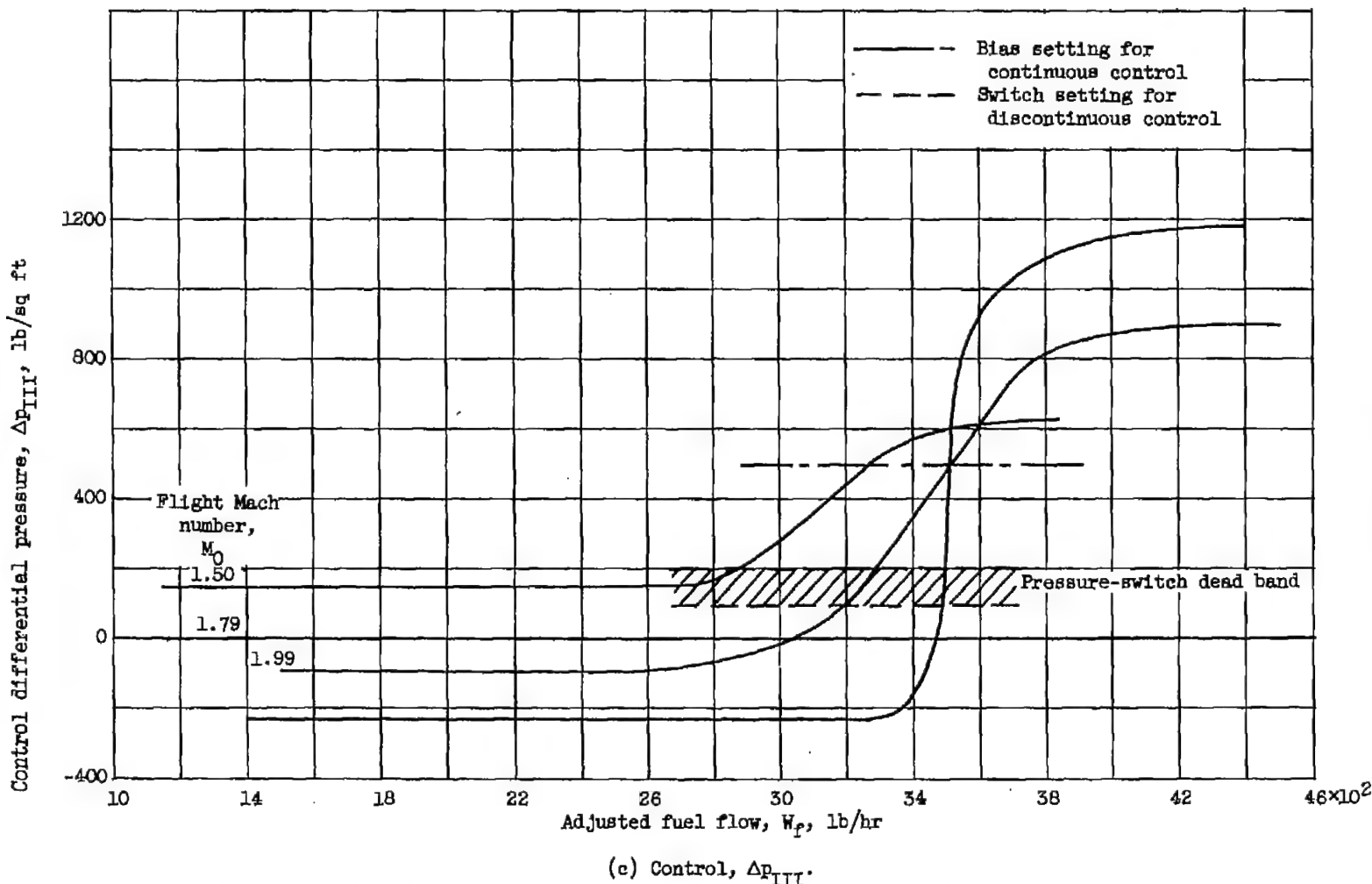
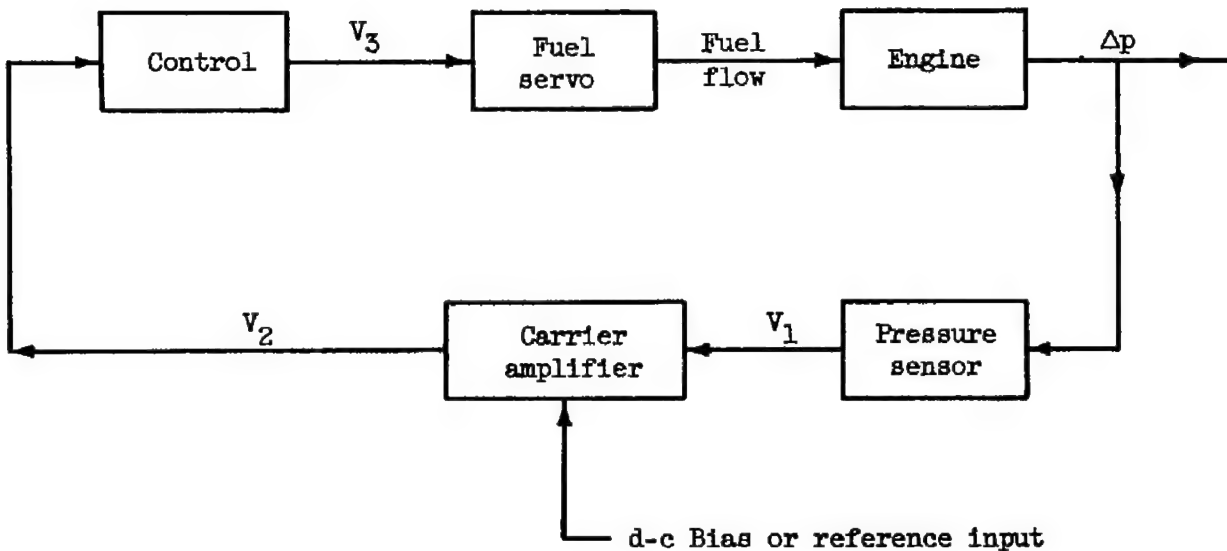
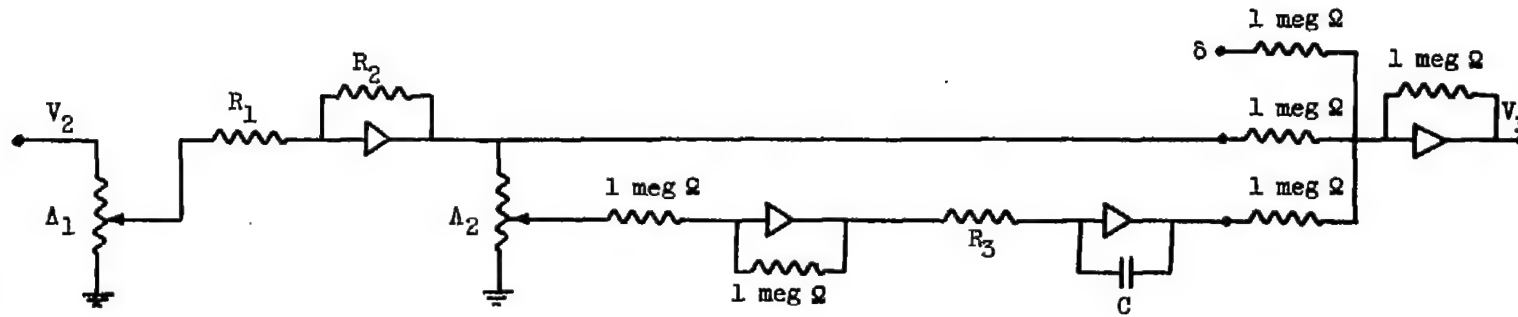


Figure 10. - Concluded. Variation of control pressure for shock-positioning controls with fuel flow at several flight Mach numbers.



(a) Block diagram.

Figure 11. - Schematic diagram of continuous-shock-positioning control system.



$$\frac{V_3}{V_2} = - A_1 \frac{R_2}{R_1} \left( 1 + \frac{1}{\frac{R_3 C_s}{A_2}} \right) \quad K = \left| A_1 \frac{R_2}{R_1} \right|$$

$$\frac{R_2}{R_1} = 10$$

$\Delta$  = Percentage of maximum  
potentiometer resistance/100

$$R_3 = 0.1 \text{ meg } \Omega$$

## ► Operational amplifier

$$C = 0.1 \mu F$$

## ► Operational amplifier

(b) Computer wiring diagram for proportional-plus-integral control.

Figure 11. - Concluded. Schematic diagram of continuous-shock-positioning control system.

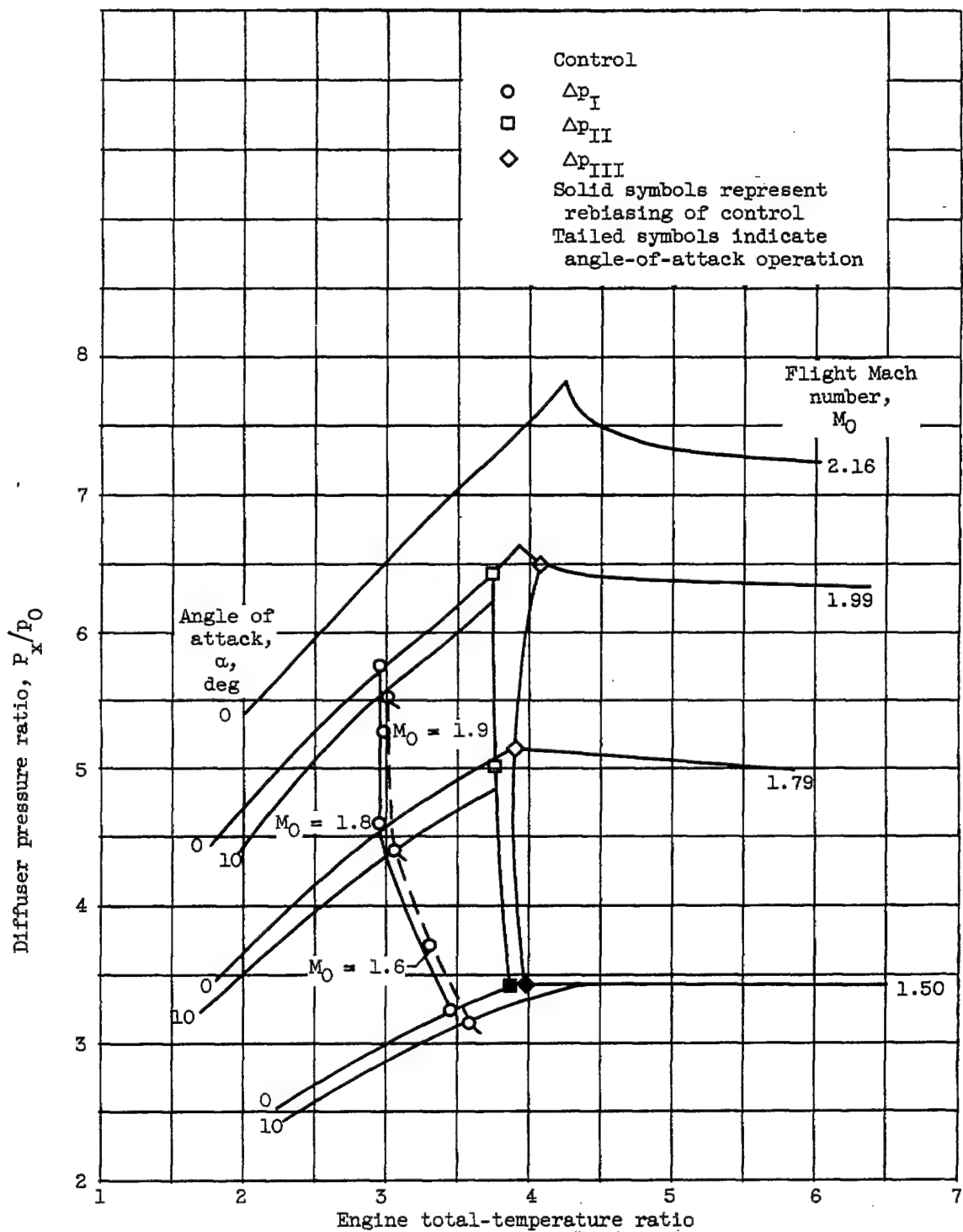
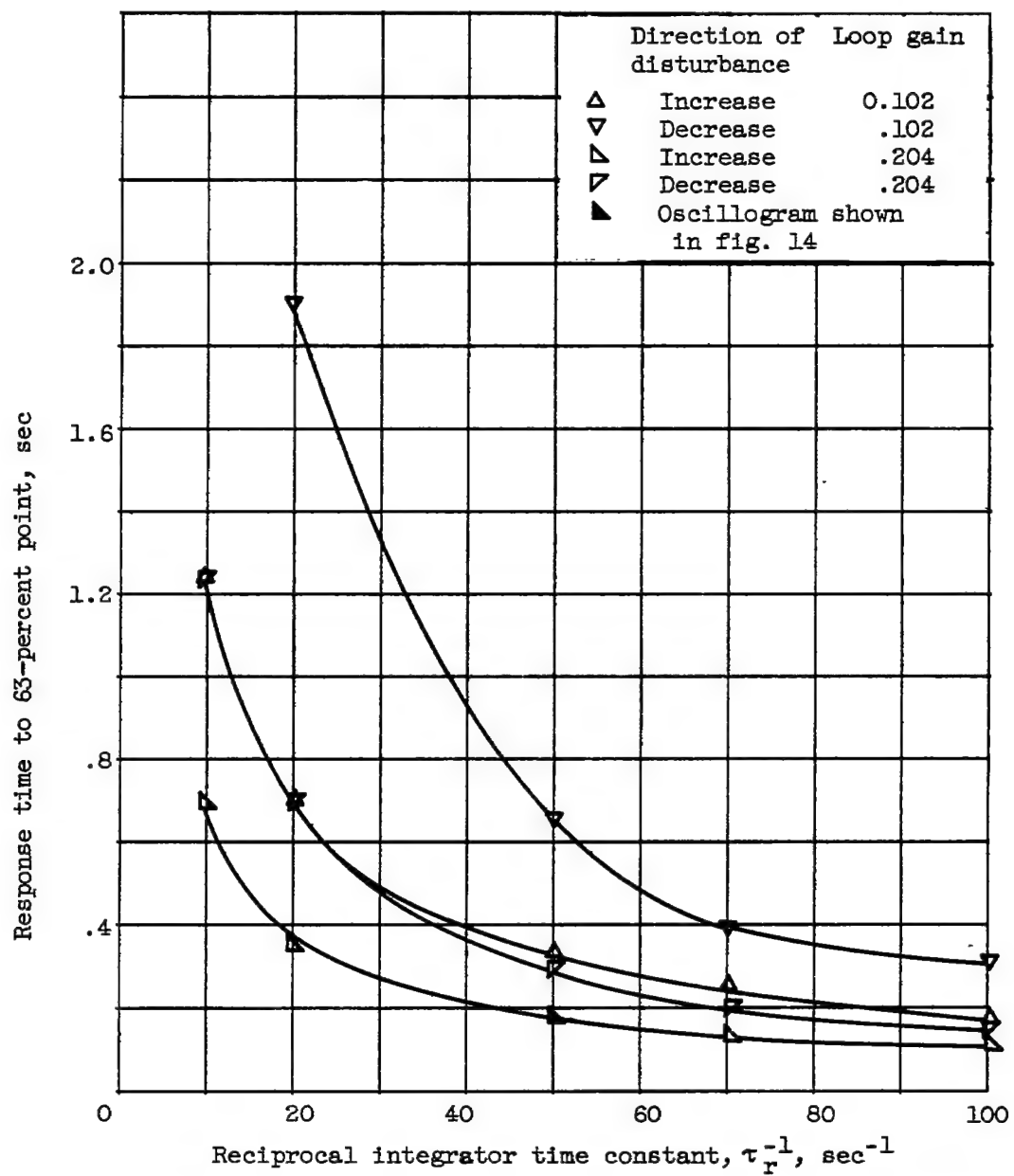
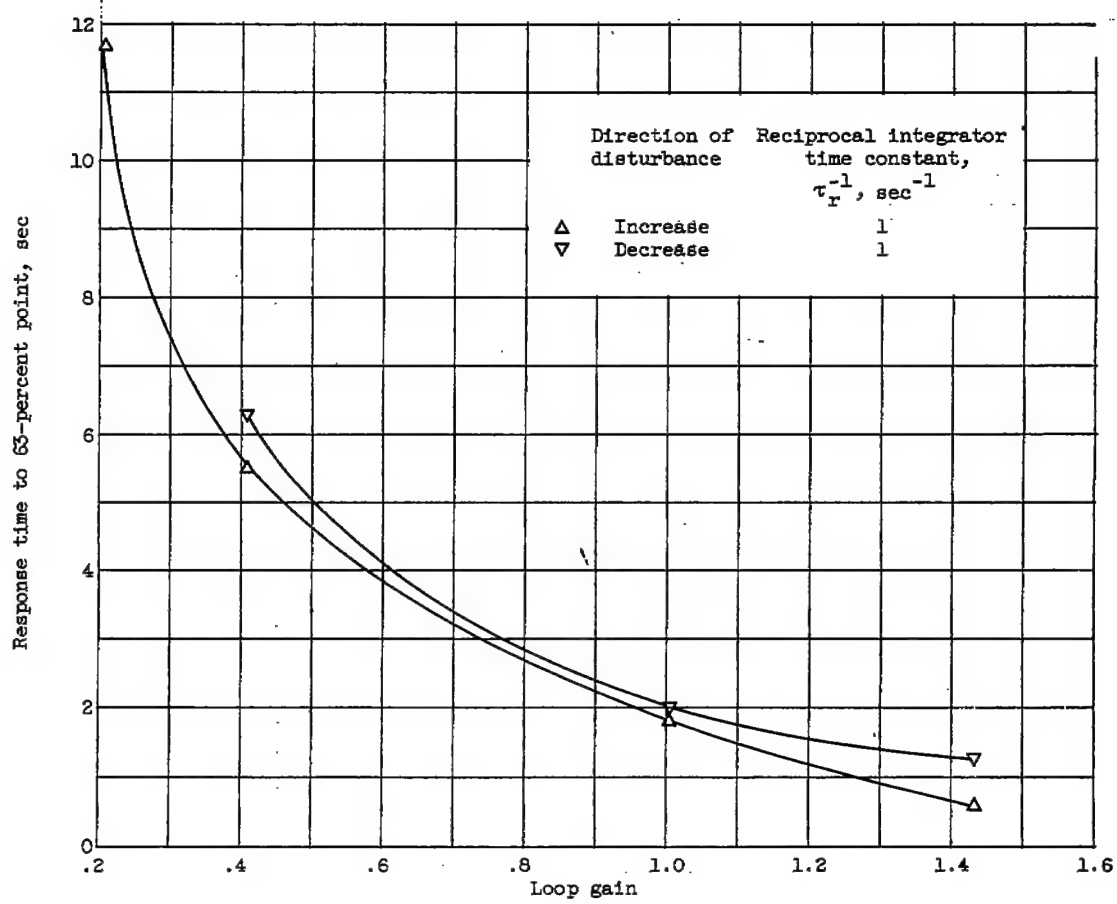


Figure 12. - Steady-state performance of three continuous-shock-positioning controls. Engine exit area  $A_6$ , 0.96 square foot.



(a) Response time as function of reciprocal integrator time constant.

Figure 13. - Dynamic response characteristics of continuous  $\Delta p_I$  control. Flight Mach number  $M_0$ , 2.0; zero angle of attack; engine-exit area  $A_6$ , 0.960 square foot; fuel flow disturbance, 556 pounds per hour.



(b) Response time as function of loop gain.

Figure 13. - Concluded. Dynamic response characteristics of continuous  $\Delta p_1$  control. Flight Mach number  $M_0$ , 2.0; zero angle of attack; engine-exit area  $A_6$ , 0.960 square foot; fuel flow disturbance, 556 pounds per hour.

CONFIDENTIAL

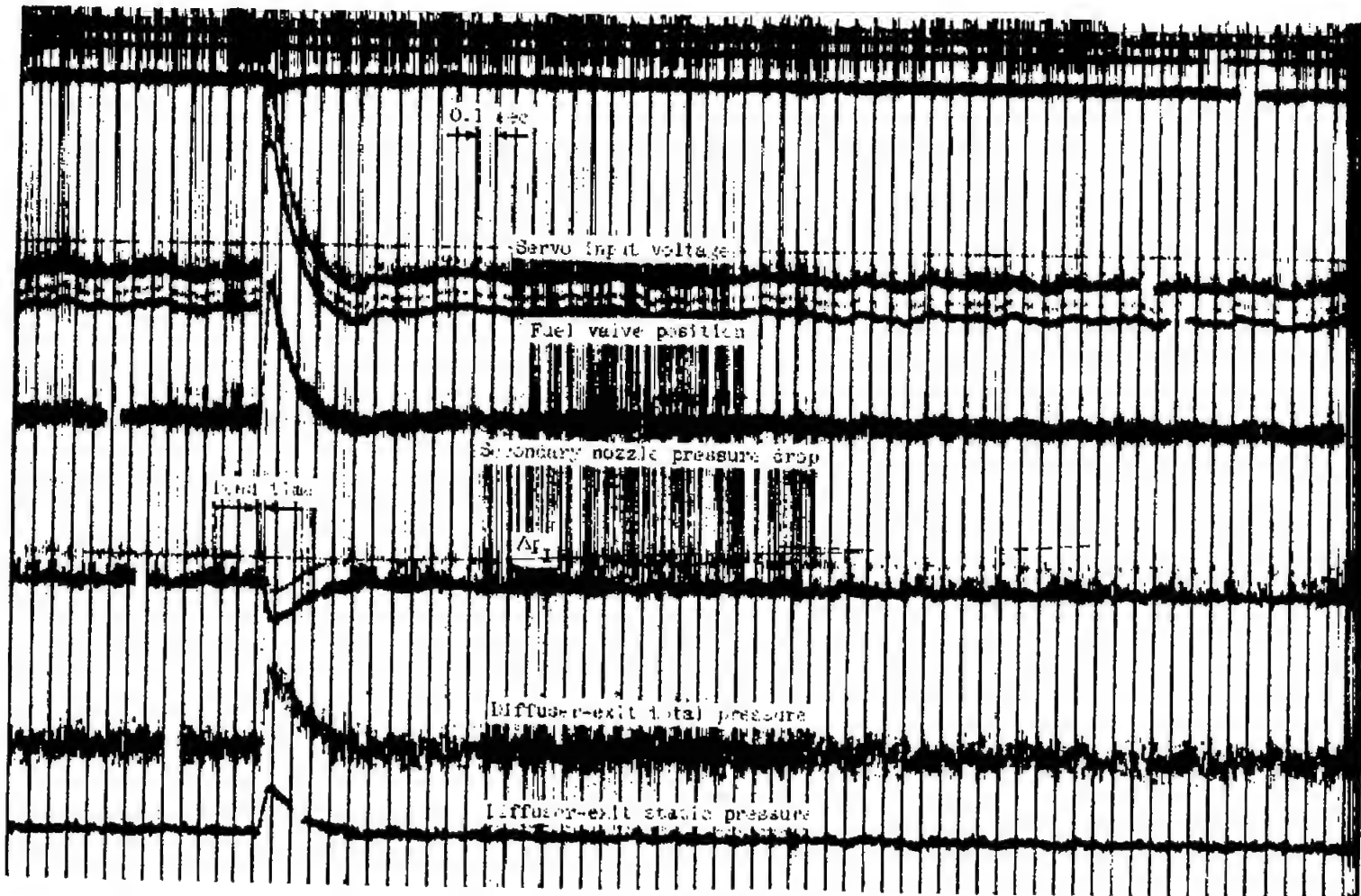
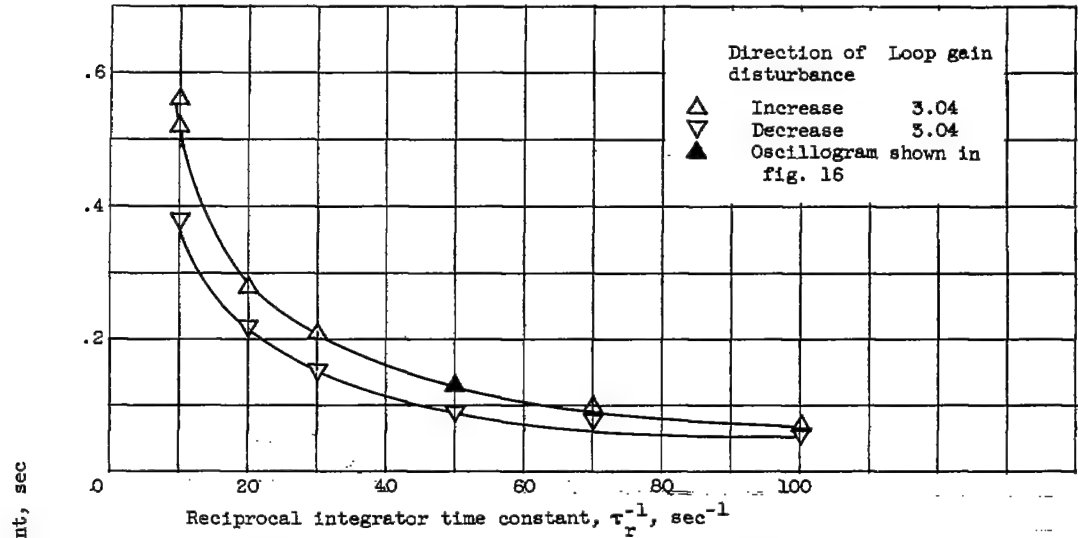
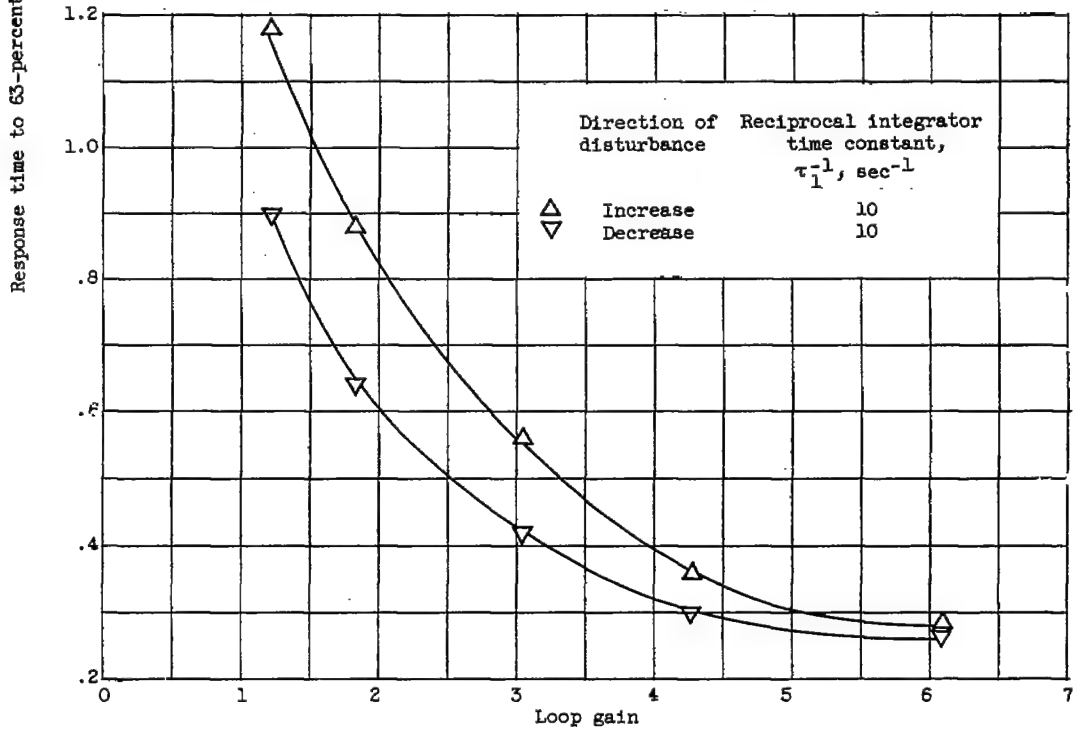


Figure 14. - Typical transient response of continuous  $\Delta p_I$  control. Flight Mach number  $M_0$ , 2.0; zero angle of attack; fuel flow disturbance, +556 pounds per hour; loop gain, 0.204; control integrator time constant, 0.05 second.



(a) Response time as function of reciprocal integrator time constant.



(b) Response time as function of loop gain.

Figure 15. - Dynamic response of continuous  $\Delta p_{III}$  control. Flight Mach number  $M_0$ , 2.0; zero angle of attack; engine-exit area  $A_6$ , 0.96 square foot; fuel flow disturbance, 278 pounds per hour.

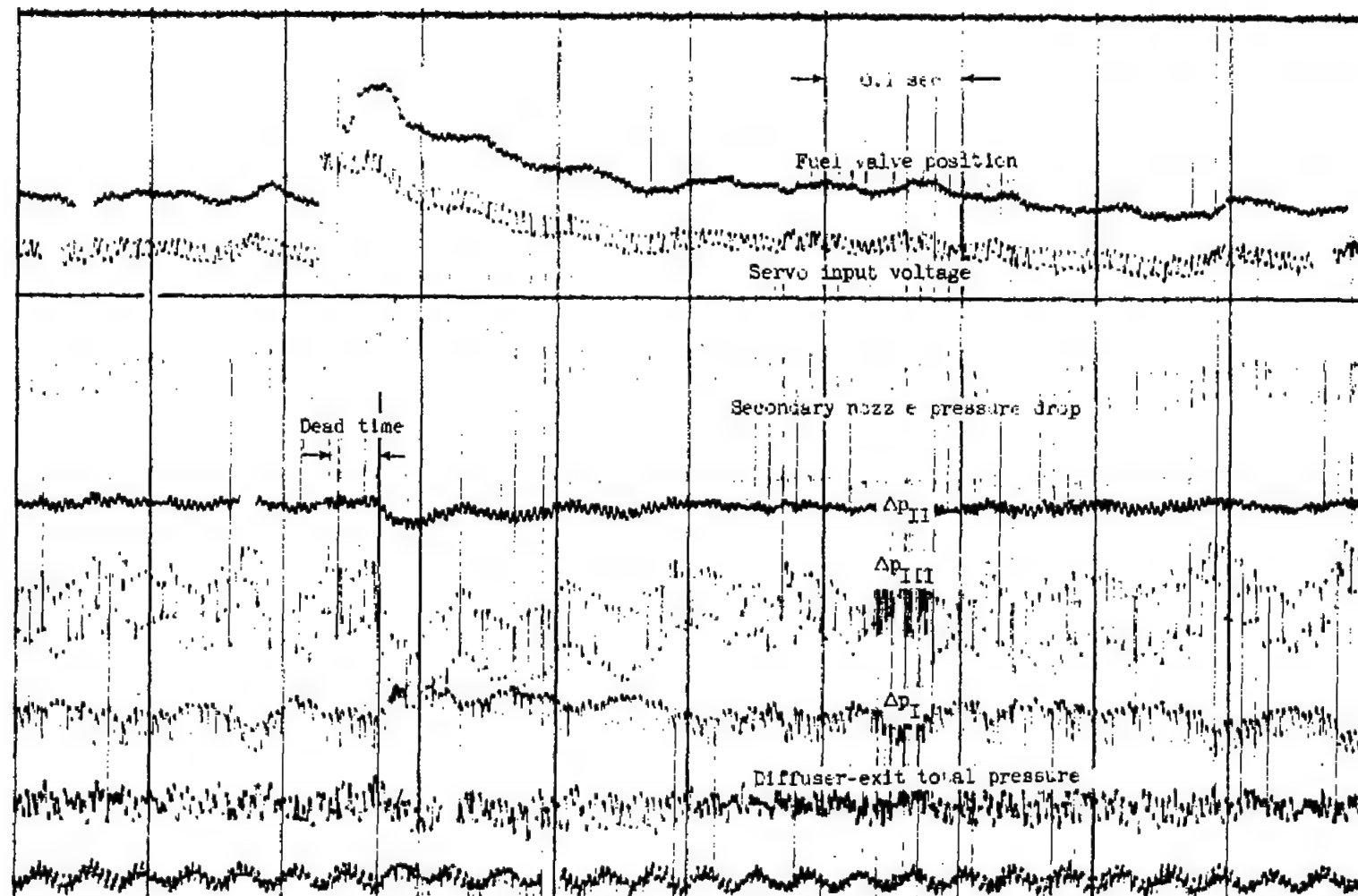


Figure 16. - Typical transient response of continuous  $\Delta p_{III}$  control. Flight Mach number  $M_0$ , 2.0; zero angle of attack; fuel flow disturbance, +278 pounds per hour; loop gain, 3.04; control integrator time constant, 0.02 second.

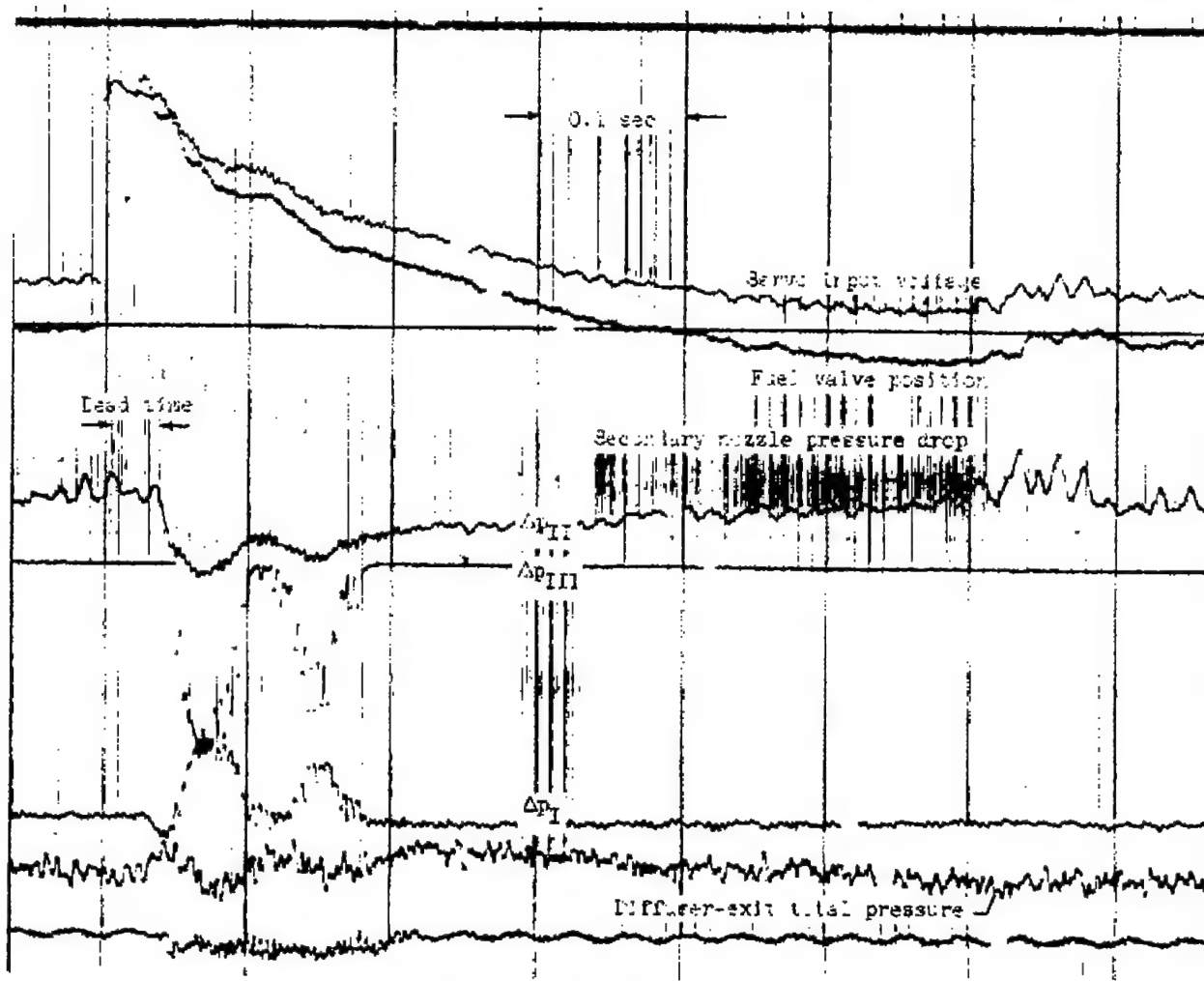
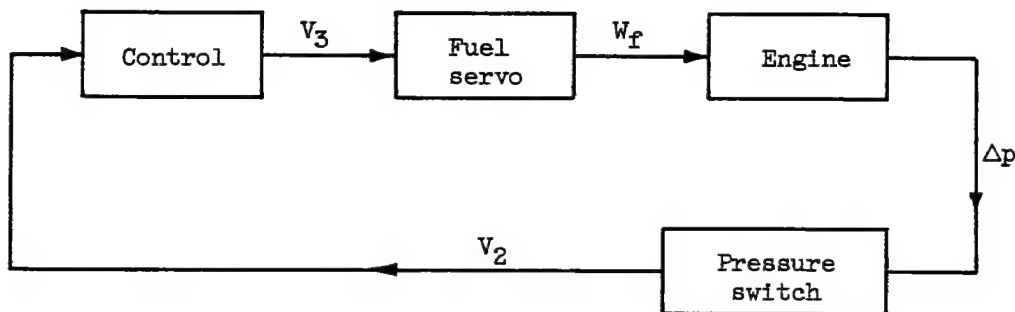


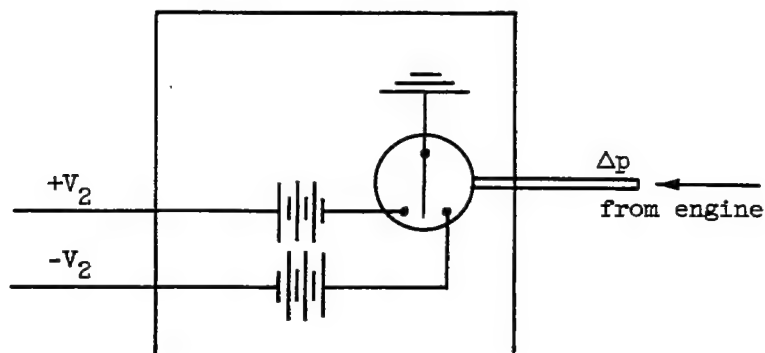
Figure 17. - Typical transient response of continuous  $\Delta p_{II}$  control. Flight Mach number  $M_0$ , 2.0; zero angle of attack; fuel flow disturbance, +556 pounds per hour; loop gain, 2.32; control integrator time constant, 0.033 second.

3409

CK-7



(a) Block diagram.



(b) Pressure switch.

Figure 18. - Schematic diagram of discontinuous-shock-positioning control.

CONFIDENTIAL

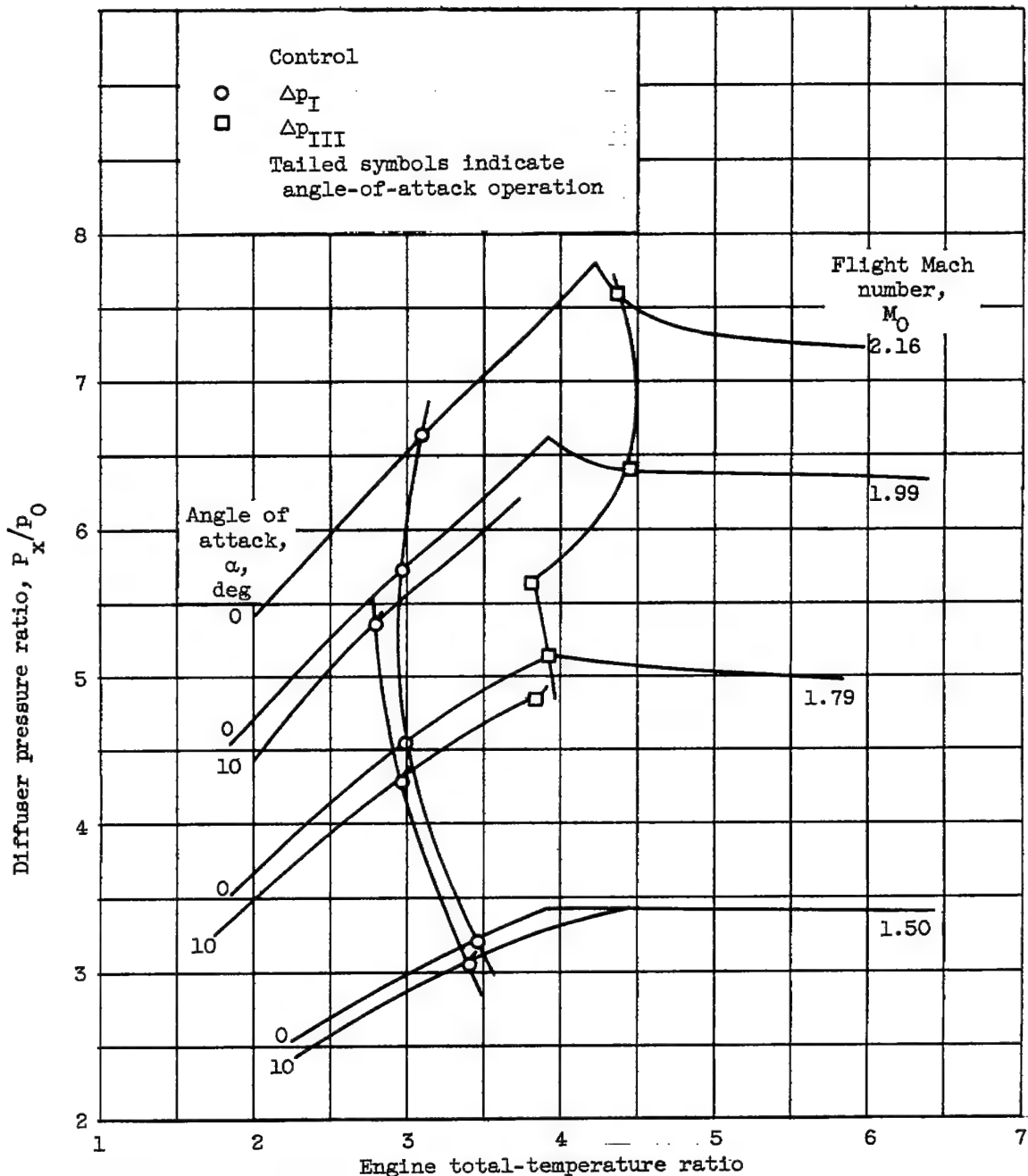


Figure 19. - Steady-state performance of discontinuous-shock-positioning controls.

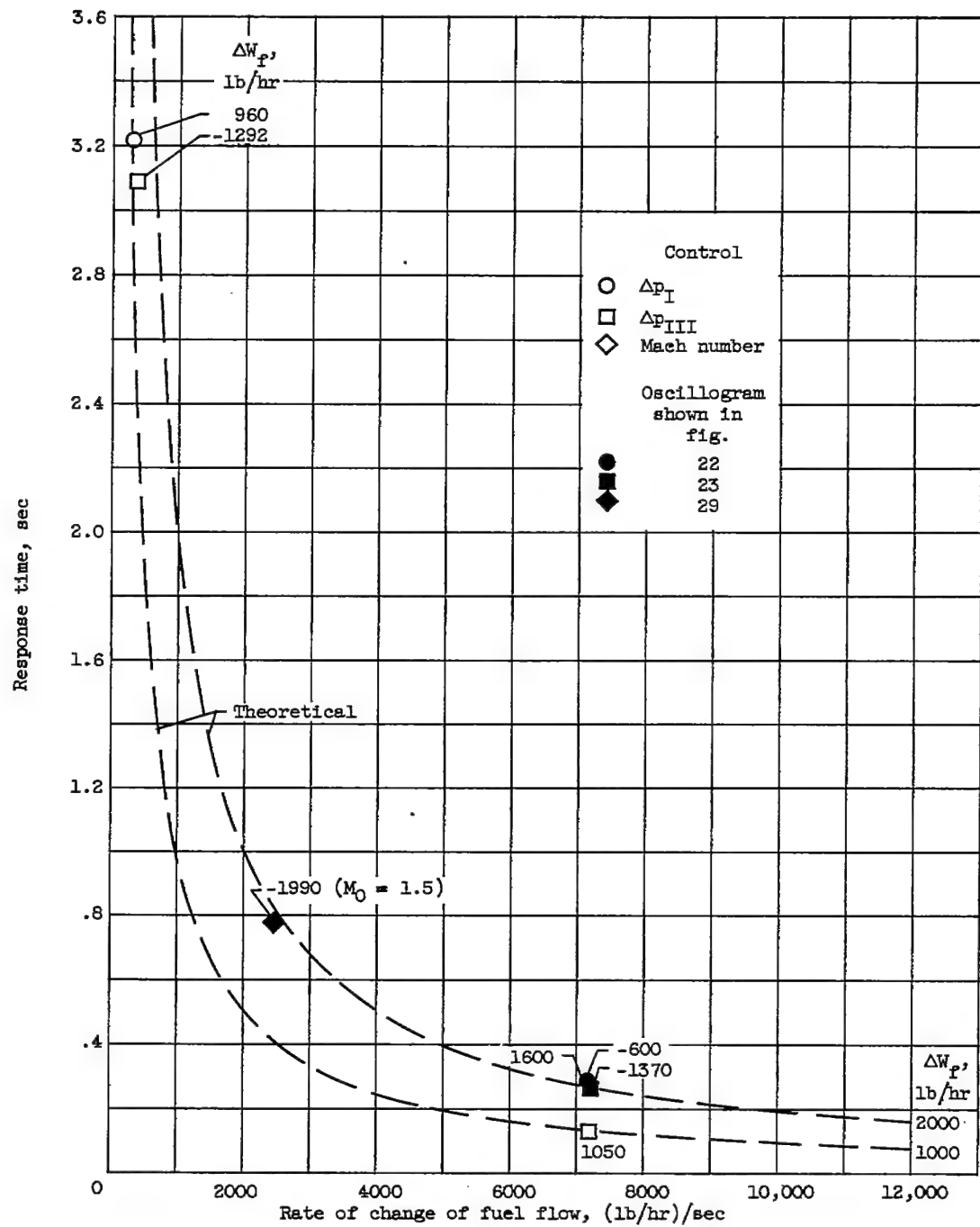


Figure 20. - Dynamic-response characteristics of discontinuous-shock-positioning controls.

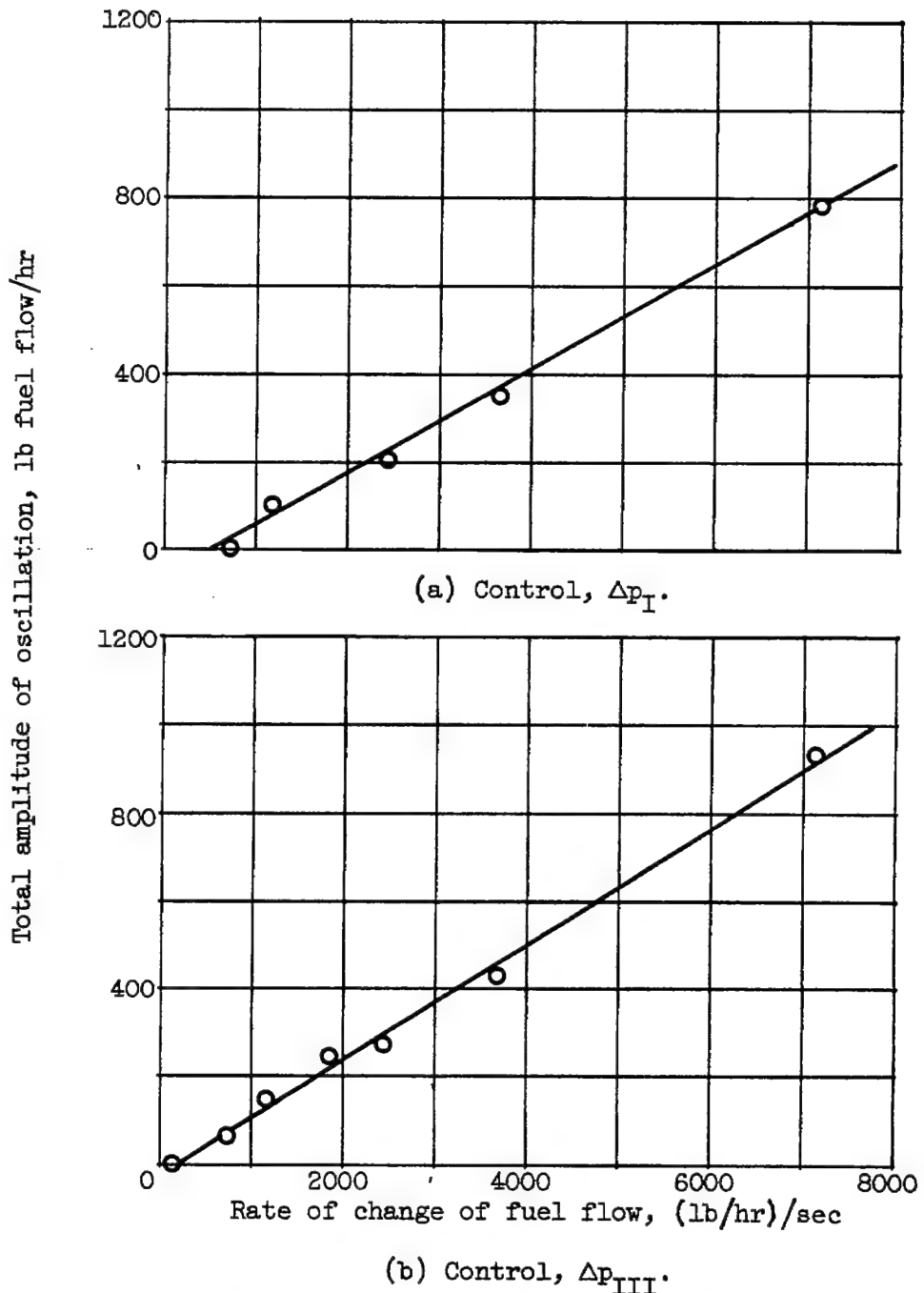


Figure 21. - Oscillation amplitudes of discontinuous-shock-positioning controls. Flight Mach number  $M_0$ , 2.0; frequency of oscillation, = 4.5 cycles per second.

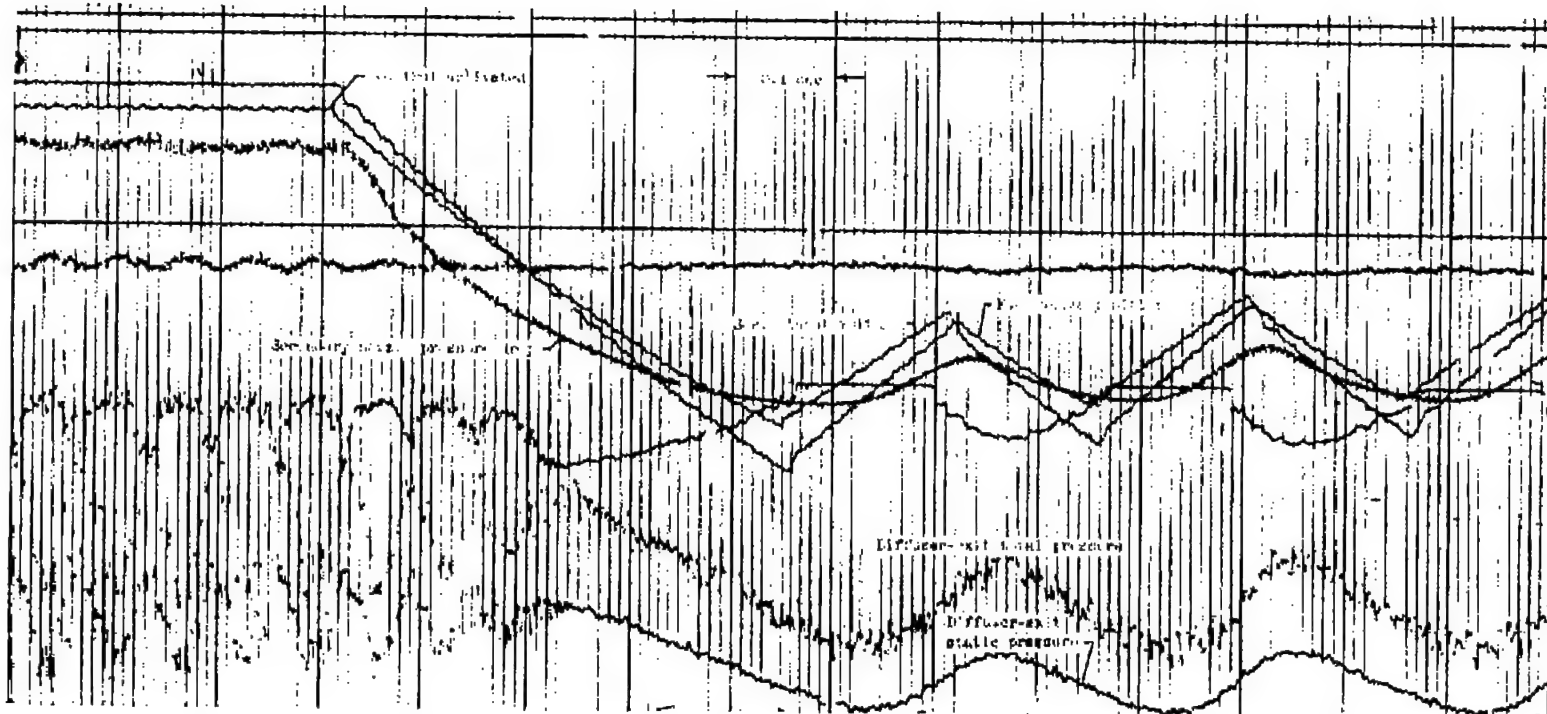


Figure 22. - Typical transient response of discontinuous  $\Delta p$  control. Flight Mach number  $M_0$ , 2.0; zero angle of attack; fuel flow displacement, + 1600 pounds per hour; rate of change of fuel flow, 7150 pounds per hour per second.

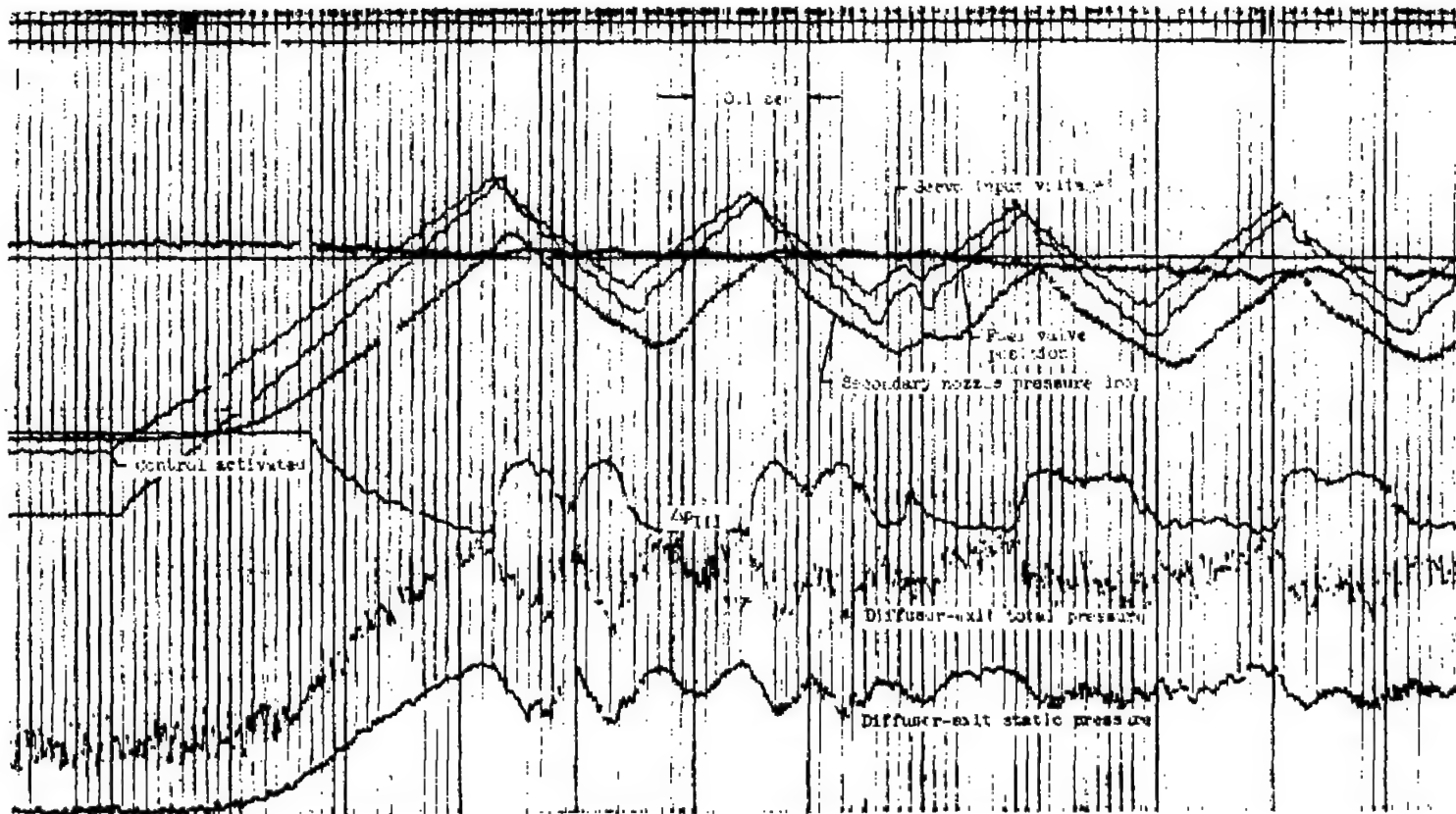
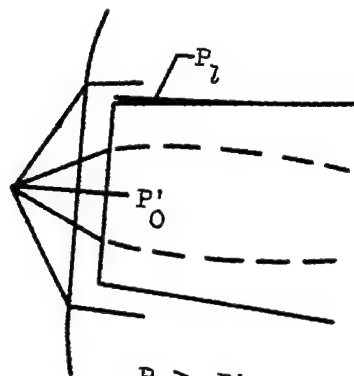
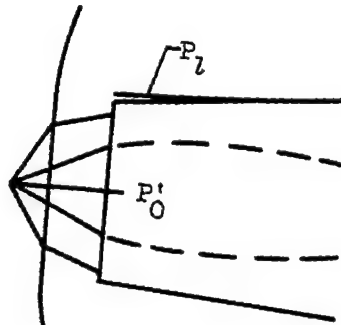


Figure 25. - Typical transient response of discontinuous Ap<sub>III</sub> control. Flight Mach number  $M_0$ , 2.0; zero angle of attack; fuel flow displacement, -1370 pounds per hour; rate of change of fuel flow, 7150 pounds per hour per second.

3409

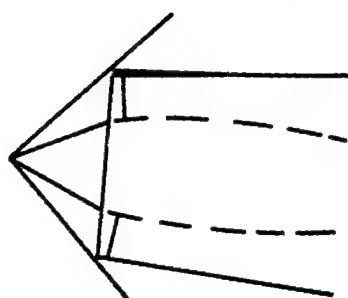


Fuel flow too low

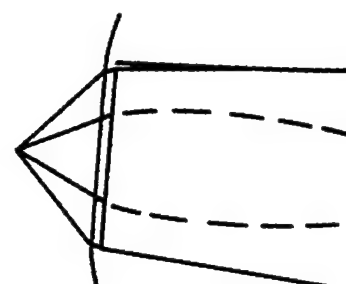


Fuel flow too high

(a) Low flight Mach number.

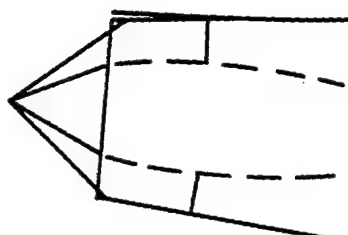


Fuel flow too low

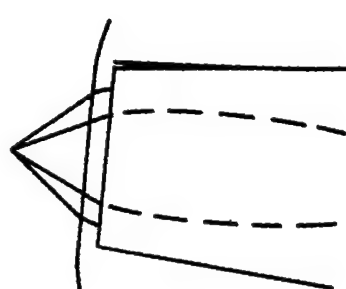


Fuel flow too high

(b) Design flight Mach number.



Diffuser supercritical

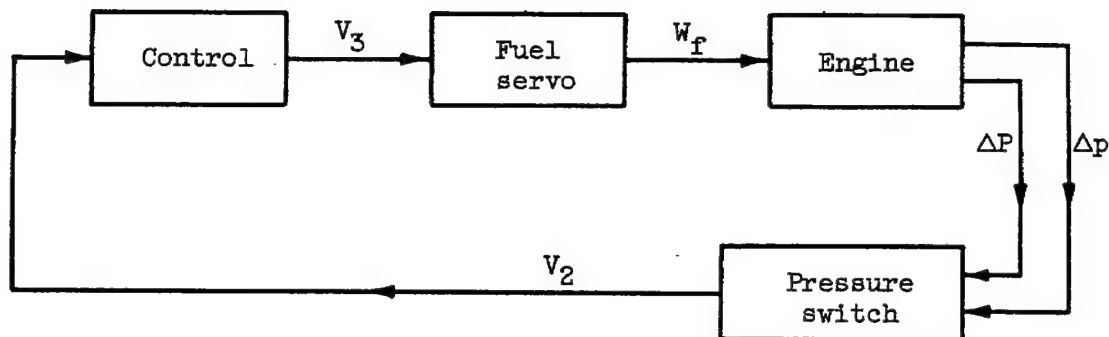


Diffuser subcritical

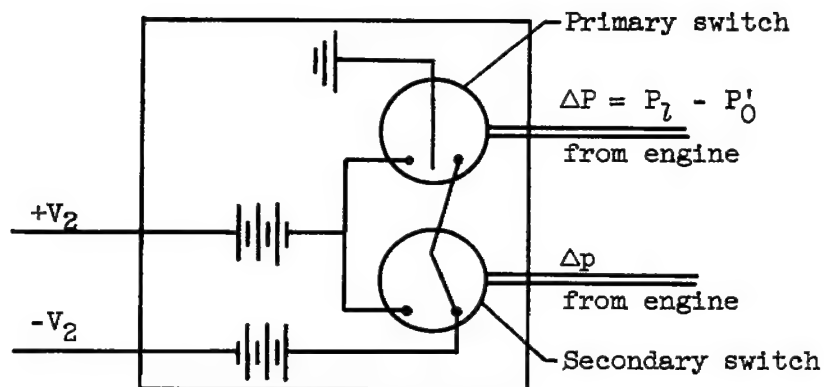
(c) Flight Mach number above design.

Figure 24. - Schematic diagram of operation of Mach number control.

IN CONFIDENTIAL



(a) Block diagram.



(b) Pressure switch.

Figure 25. - Block and pressure-switch diagram of Mach number control.

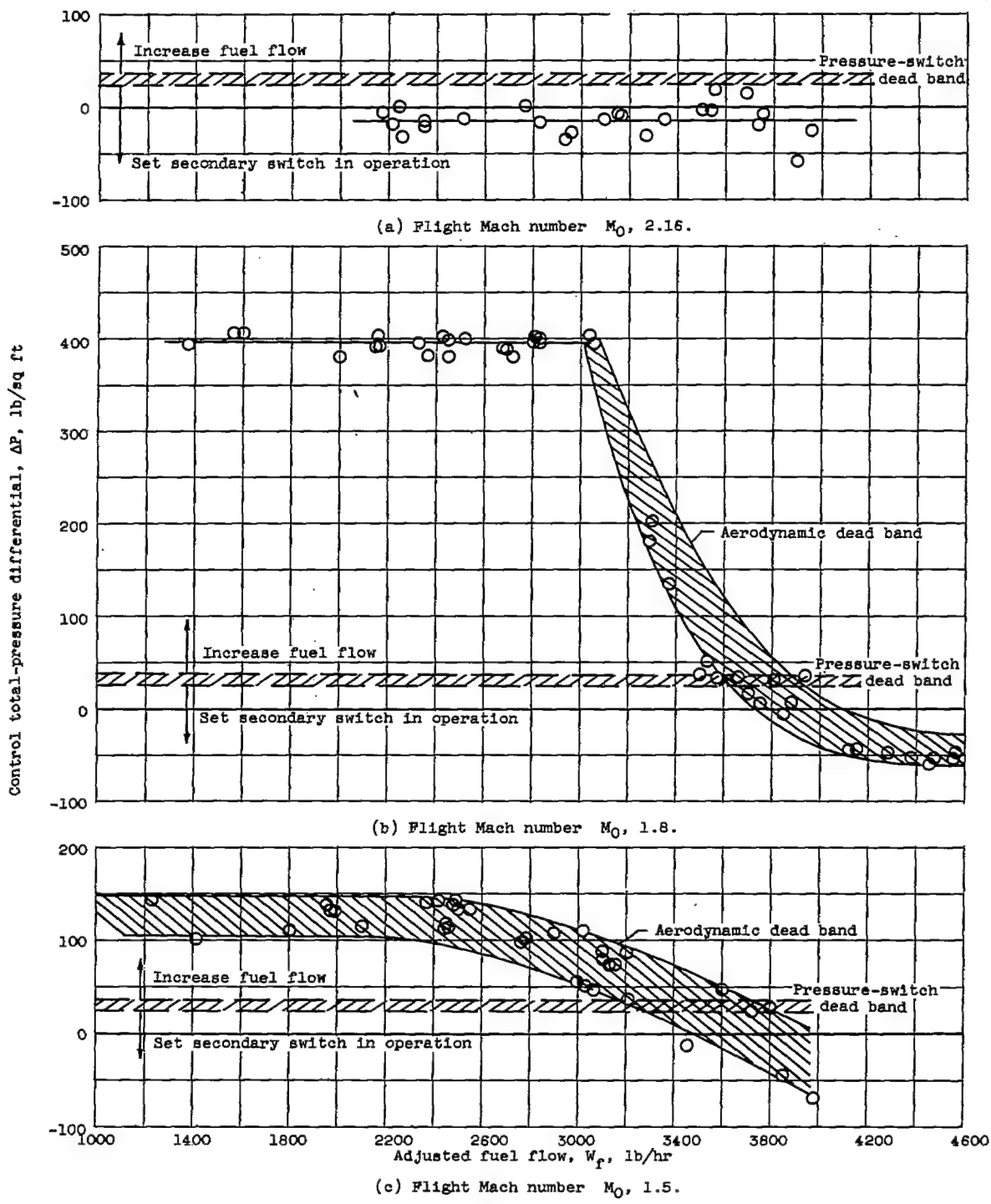


Figure 26. - Control pressure for Mach number control.

CONFIDENTIAL

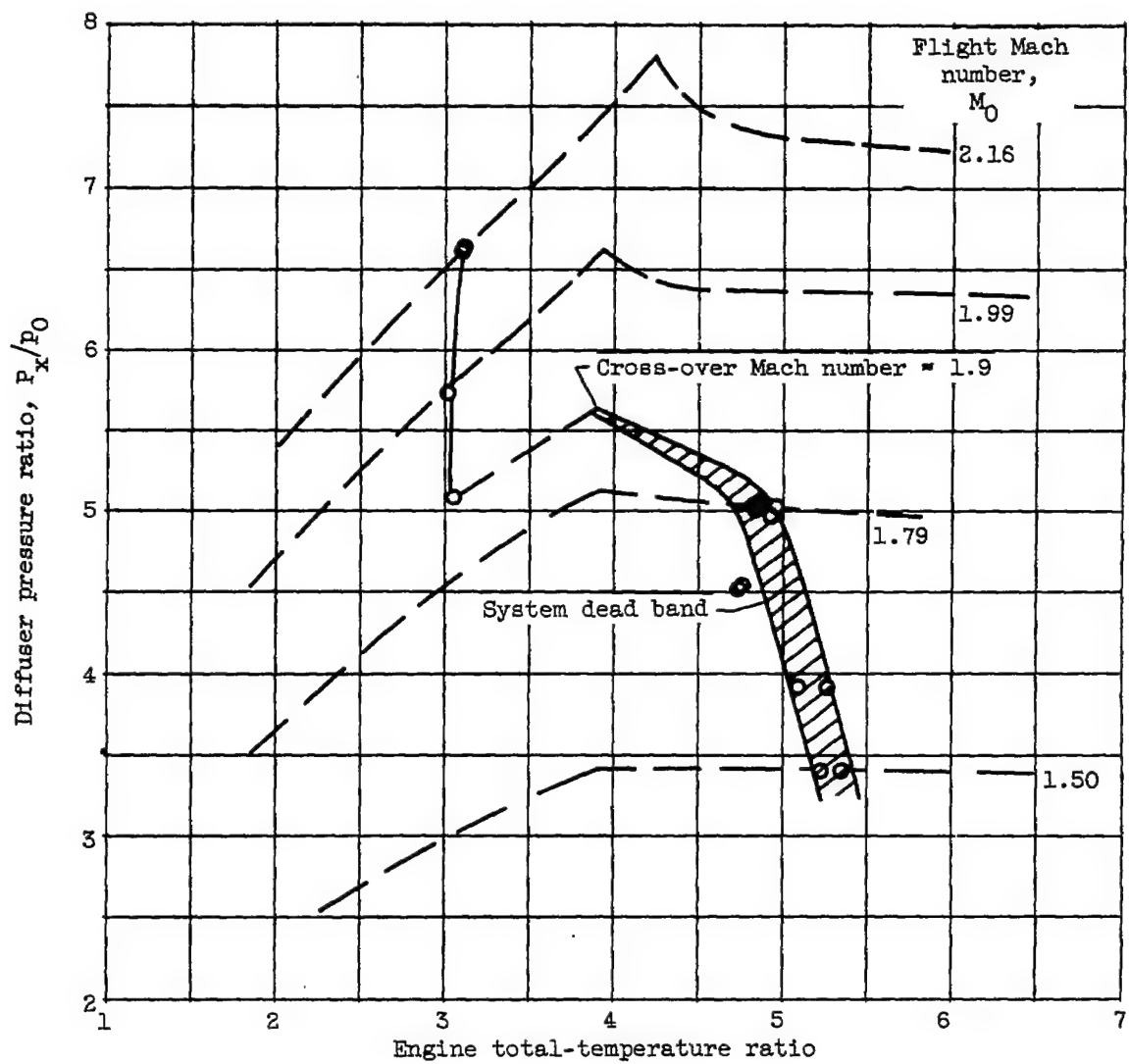


Figure 27. - Steady-state performance of Mach number control.

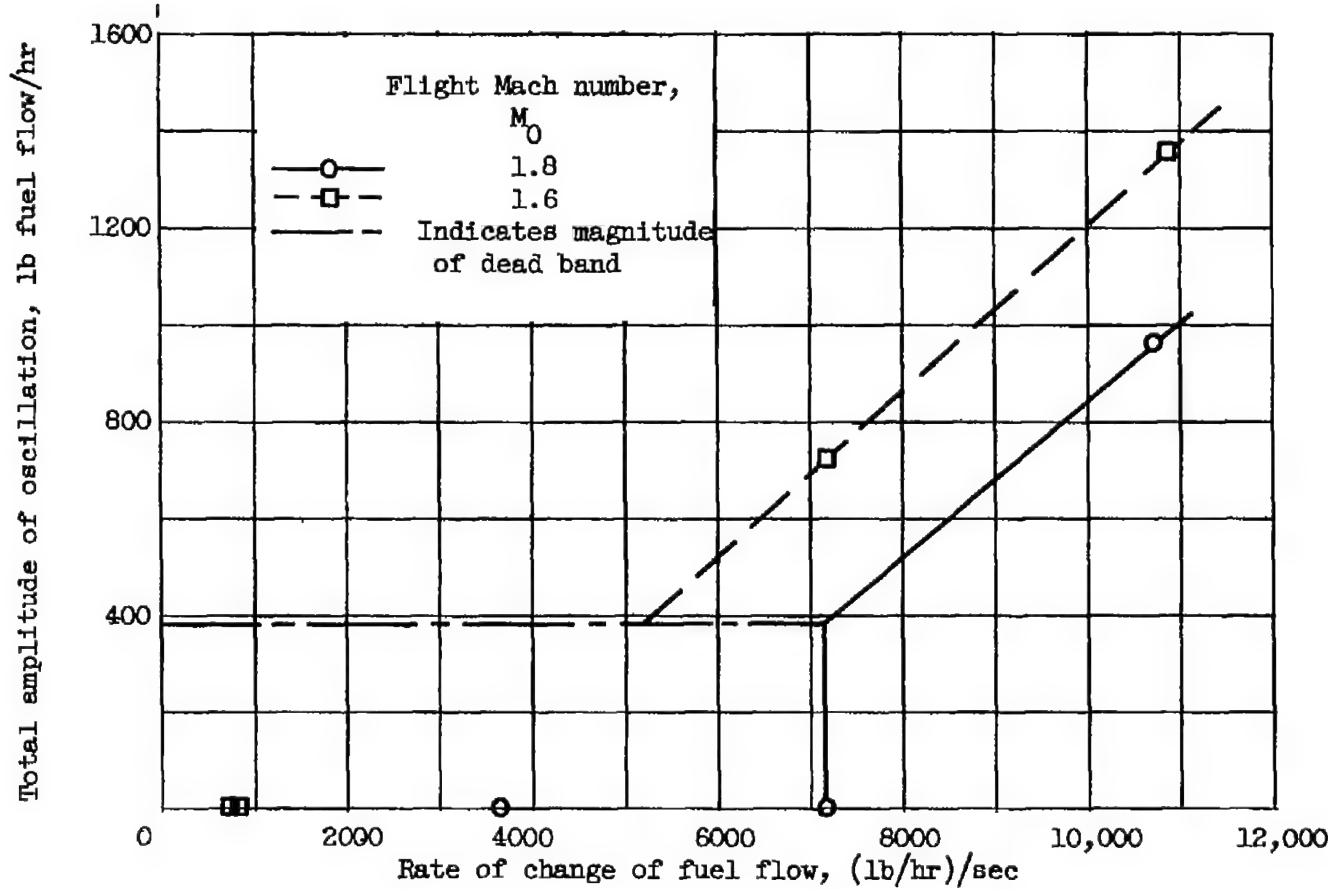


Figure 28. - Oscillation amplitudes for Mach number control.

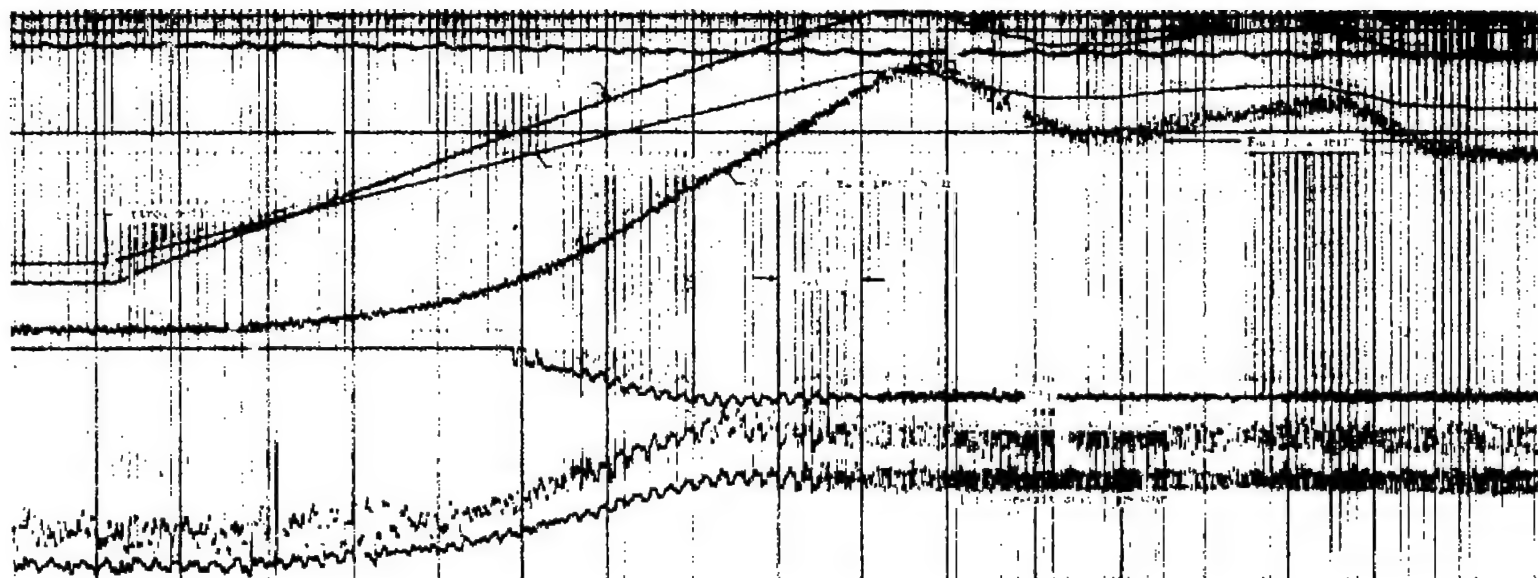


Figure 29. - Typical transient response of shock-positioning Mach number control. Flight Mach number  $M_0$ , 1.5; zero angle of attack; fuel flow displacement, -1990 pounds per hour; rate of change of fuel flow, 2450 pounds per hour per second.

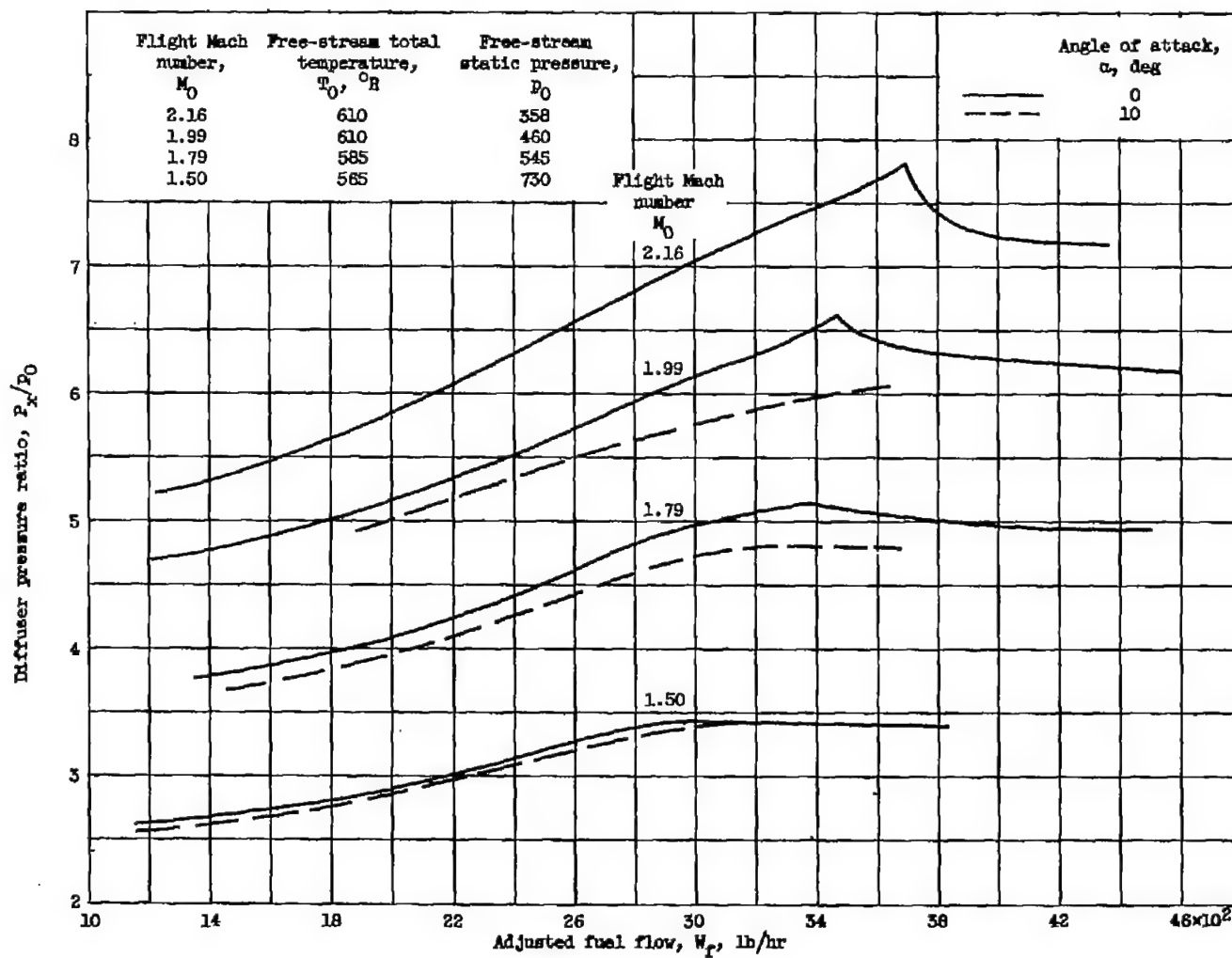


Figure 30. - Variation of diffuser pressure ratio with fuel flow at several flight Mach numbers. Engine-exit area  $A_0$ , 0.96 square foot.

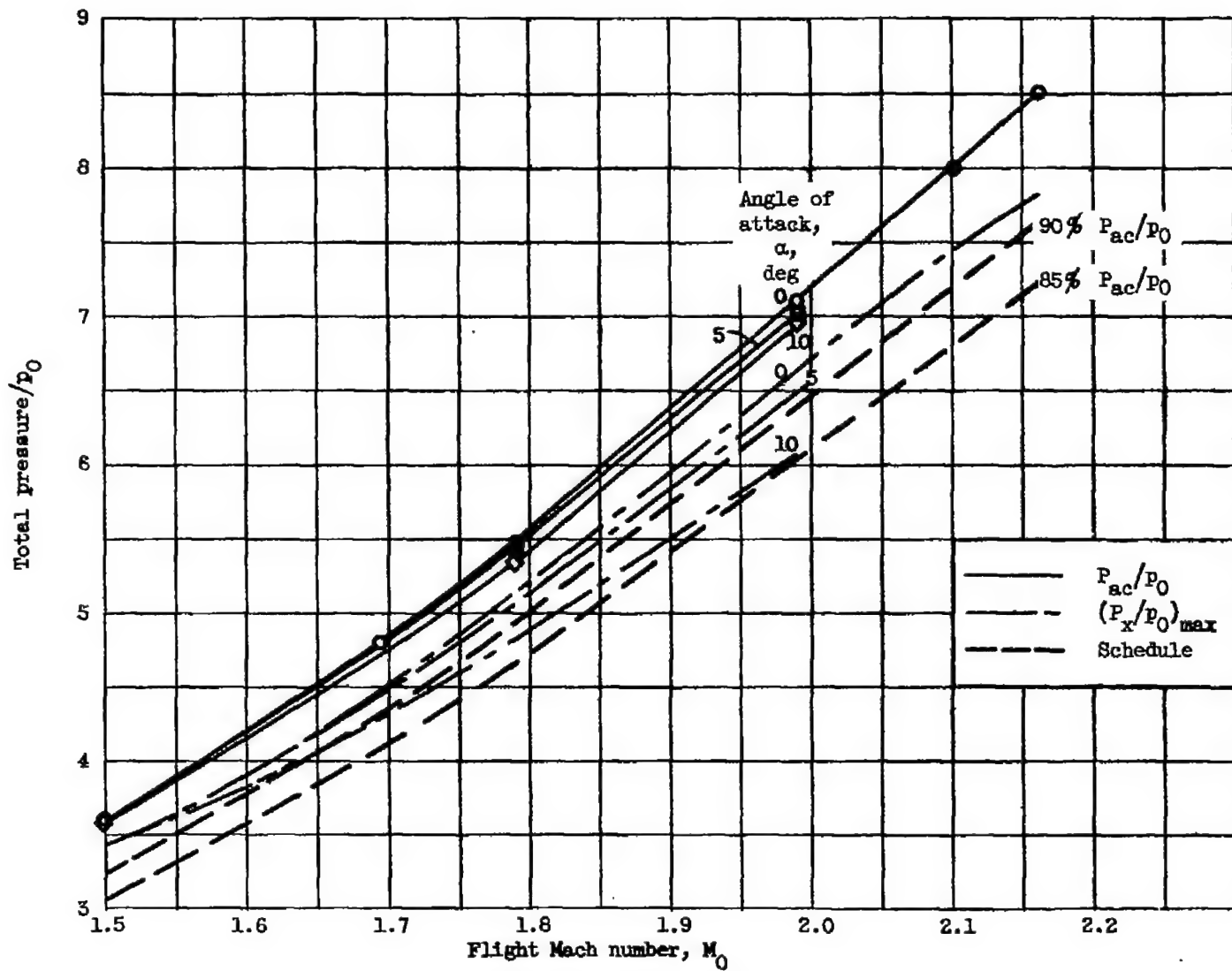


Figure 31. - Variation of  $P_{ac}/p_0$  and  $(P_x/p_0)_{max}$  with flight Mach number and angle of attack.

TOP SECRET//COMINT

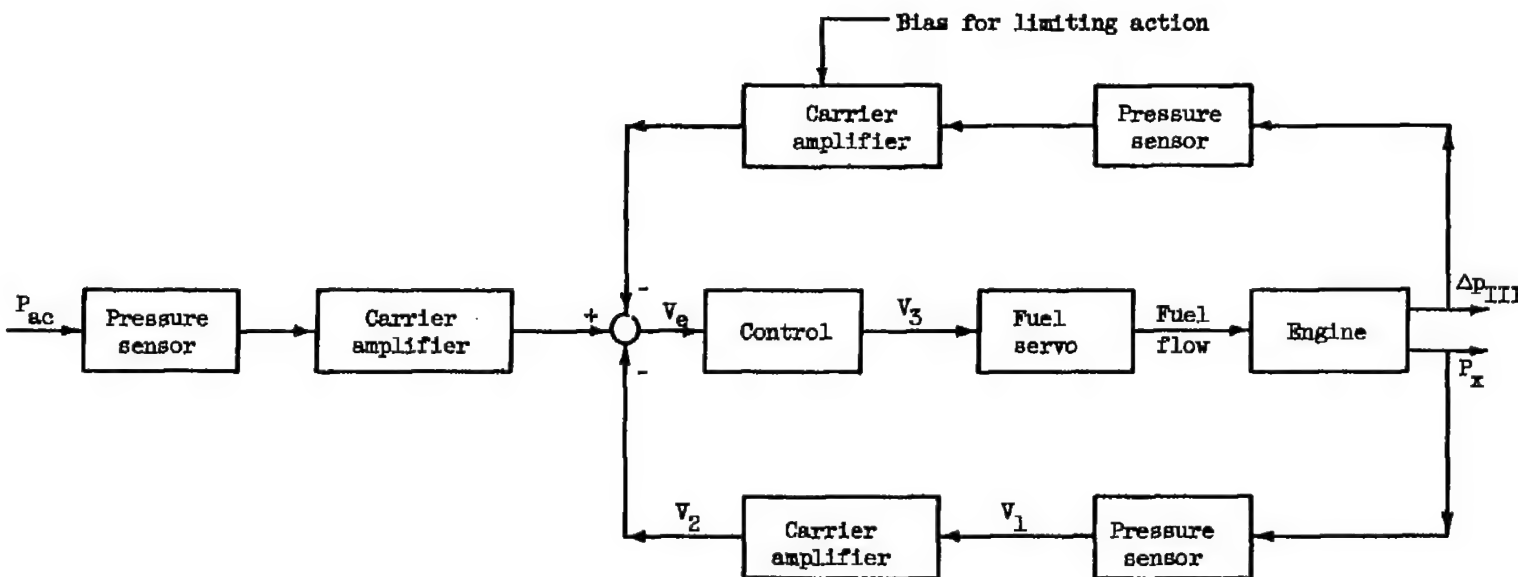


Figure 32. - Block diagram of diffuser pressure control with input schedule computer and shock-position limiter.

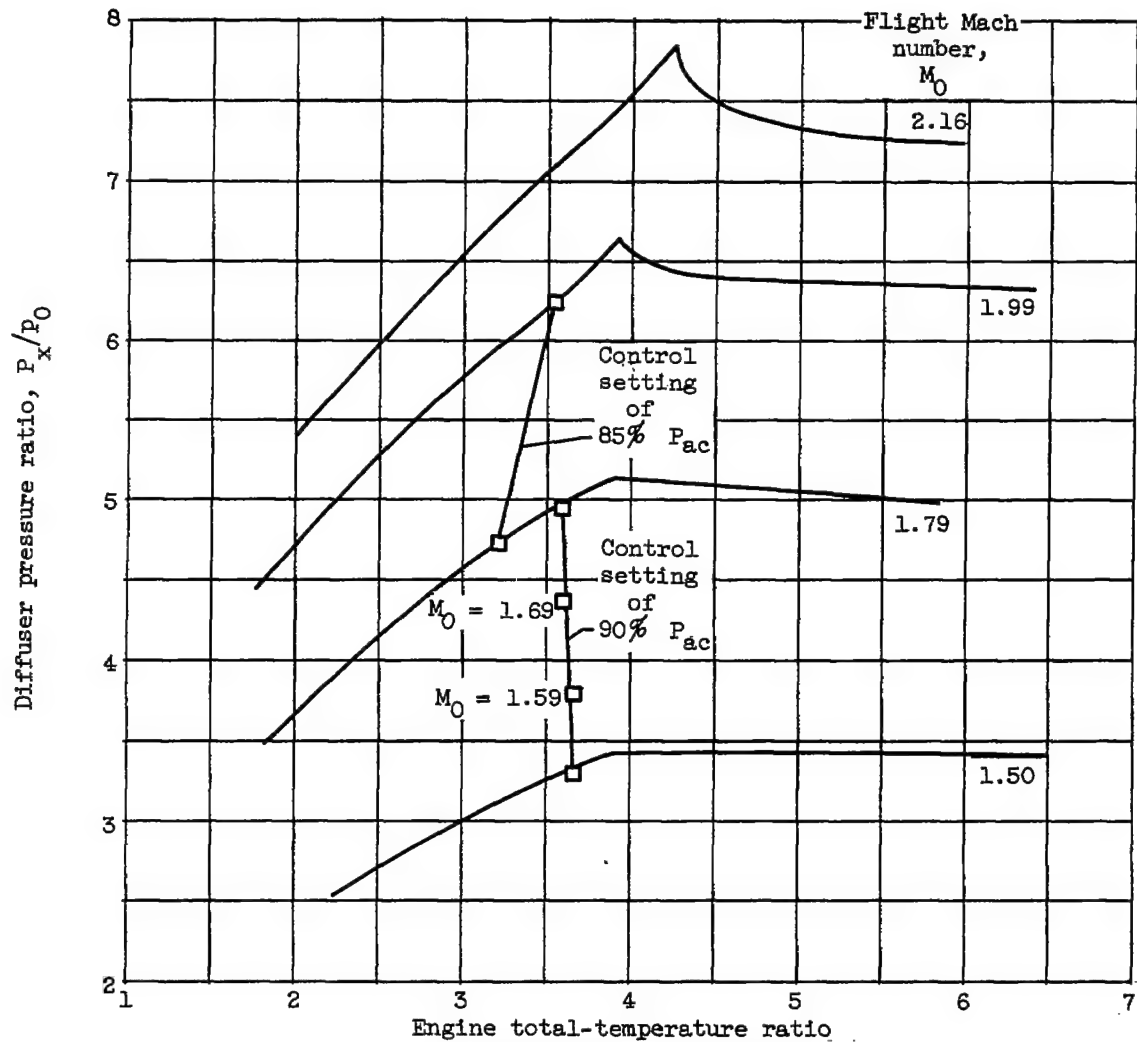
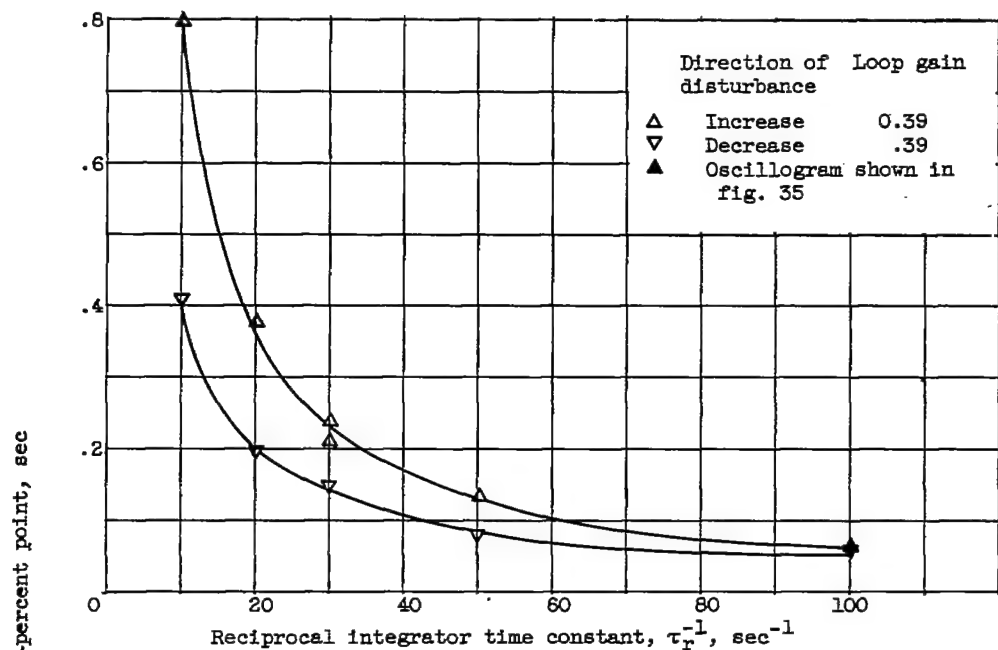


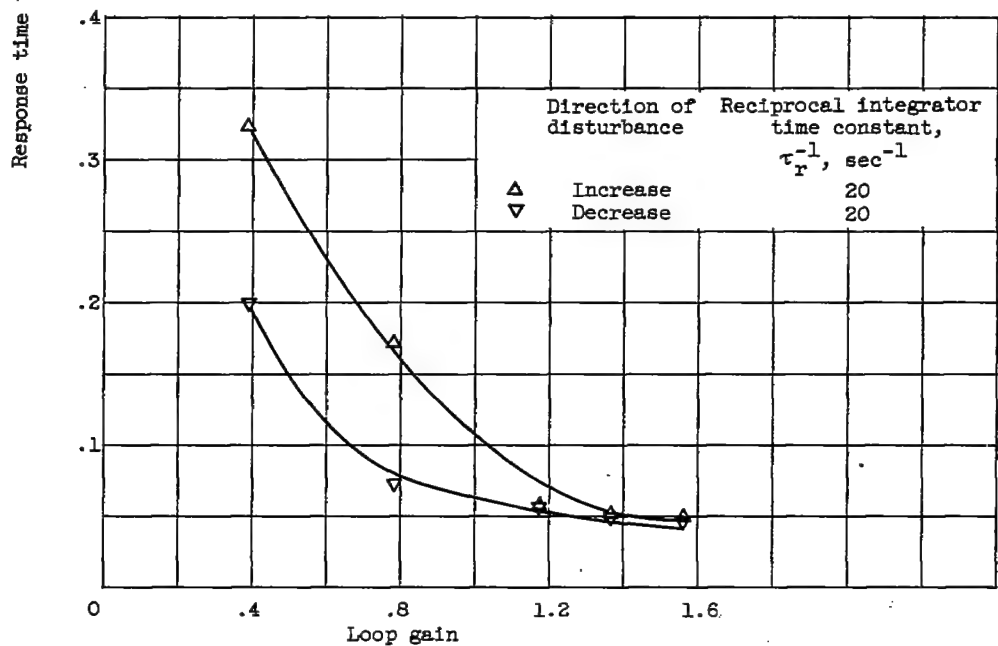
Figure 33. - Steady-state performance of diffuser pressure control.  
Engine exit area  $A_6$ , 0.96 square foot; zero angle of attack.

CONFIDENTIAL

3409



(a) Response time as function of reciprocal integrator time constant.



(b) Response time as function of loop gain.

Figure 34. - Dynamic response of diffuser pressure control. Flight Mach number  $M_0$ , 1.5; zero angle of attack; engine-exit area  $A_6$ , 0.96 square foot; fuel flow disturbance, 5556 pounds per hour.

CONFIDENTIAL

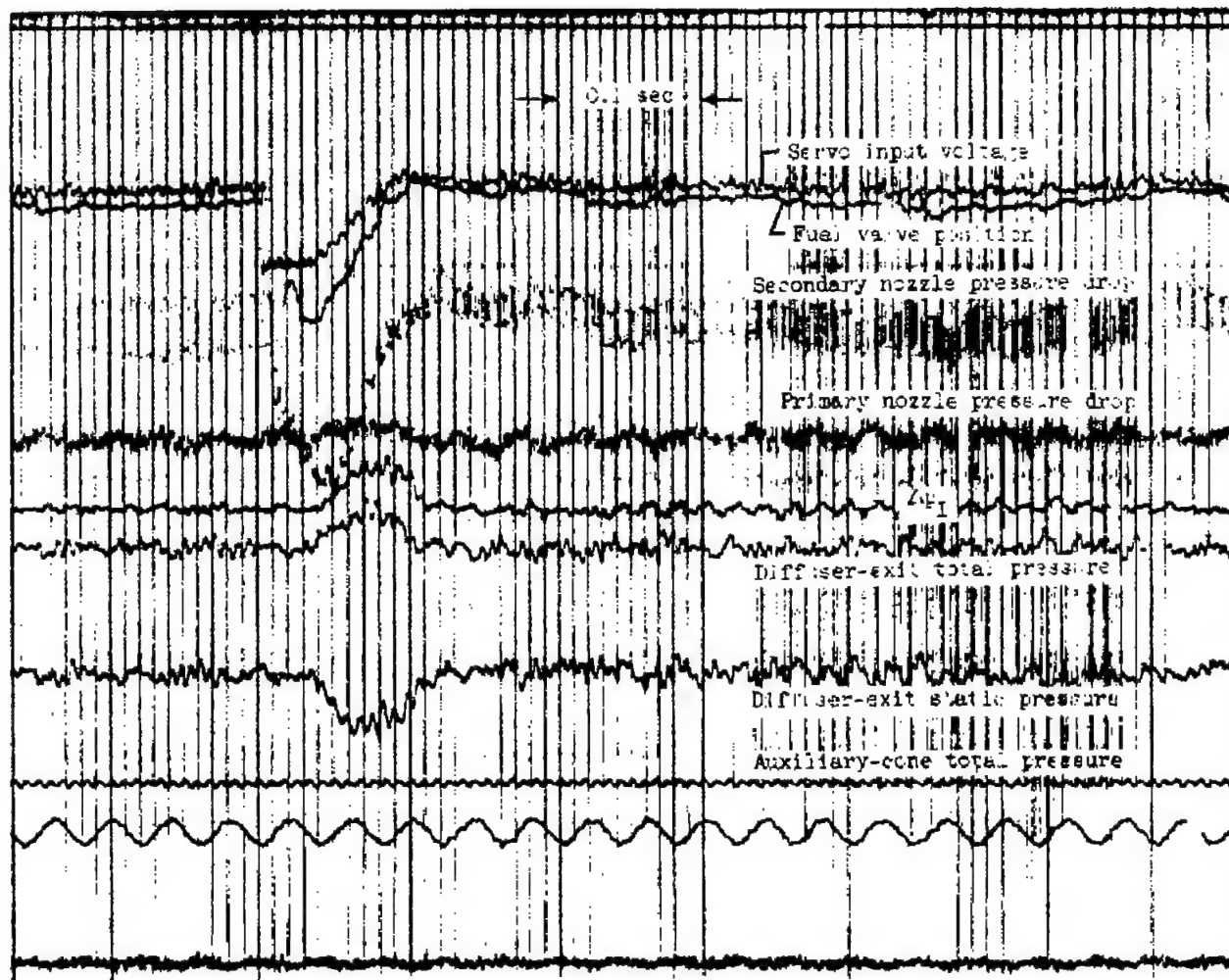


Figure 35. - Typical response of diffuser-exit pressure scheduling control. Flight Mach number  $M_\infty$ , 1.5; zero angle of attack; fuel flow disturbance, -556 pounds per hour; loop gain, 0.39; control integrator time constant, 0.01 second.

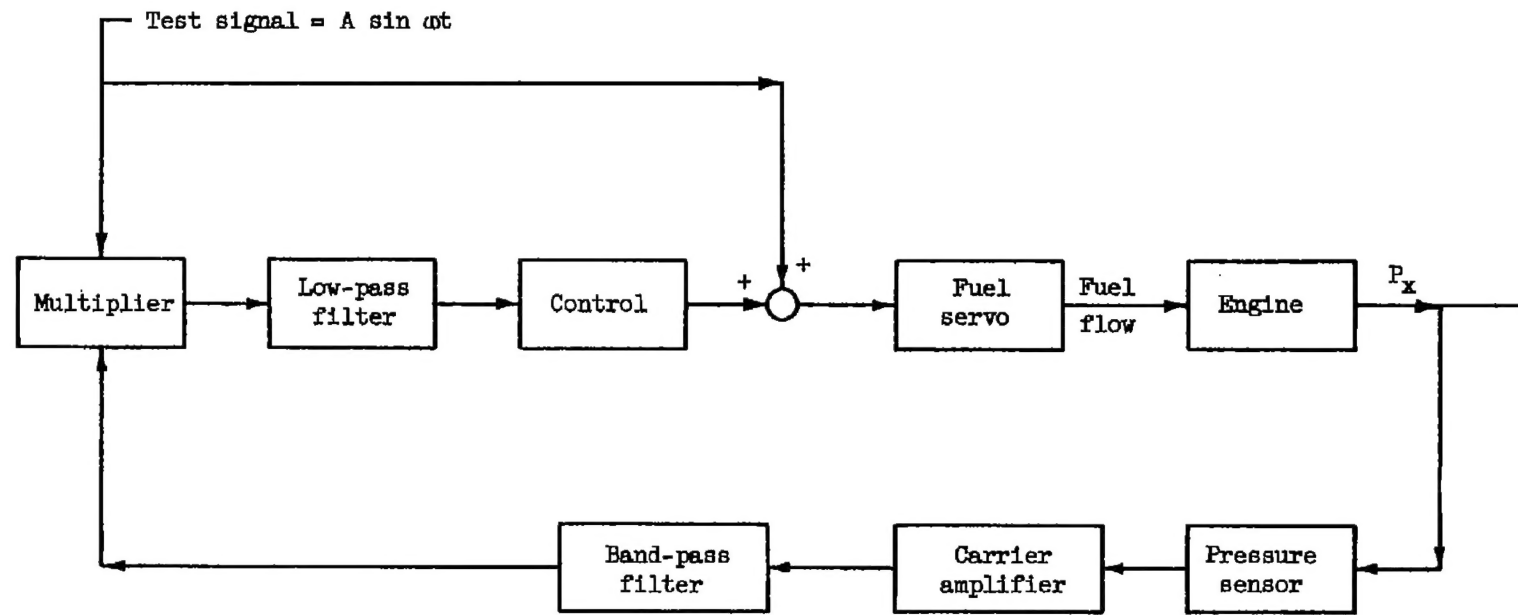


Figure 36. - Block diagram of optimalizer control for diffuser pressure.

6072

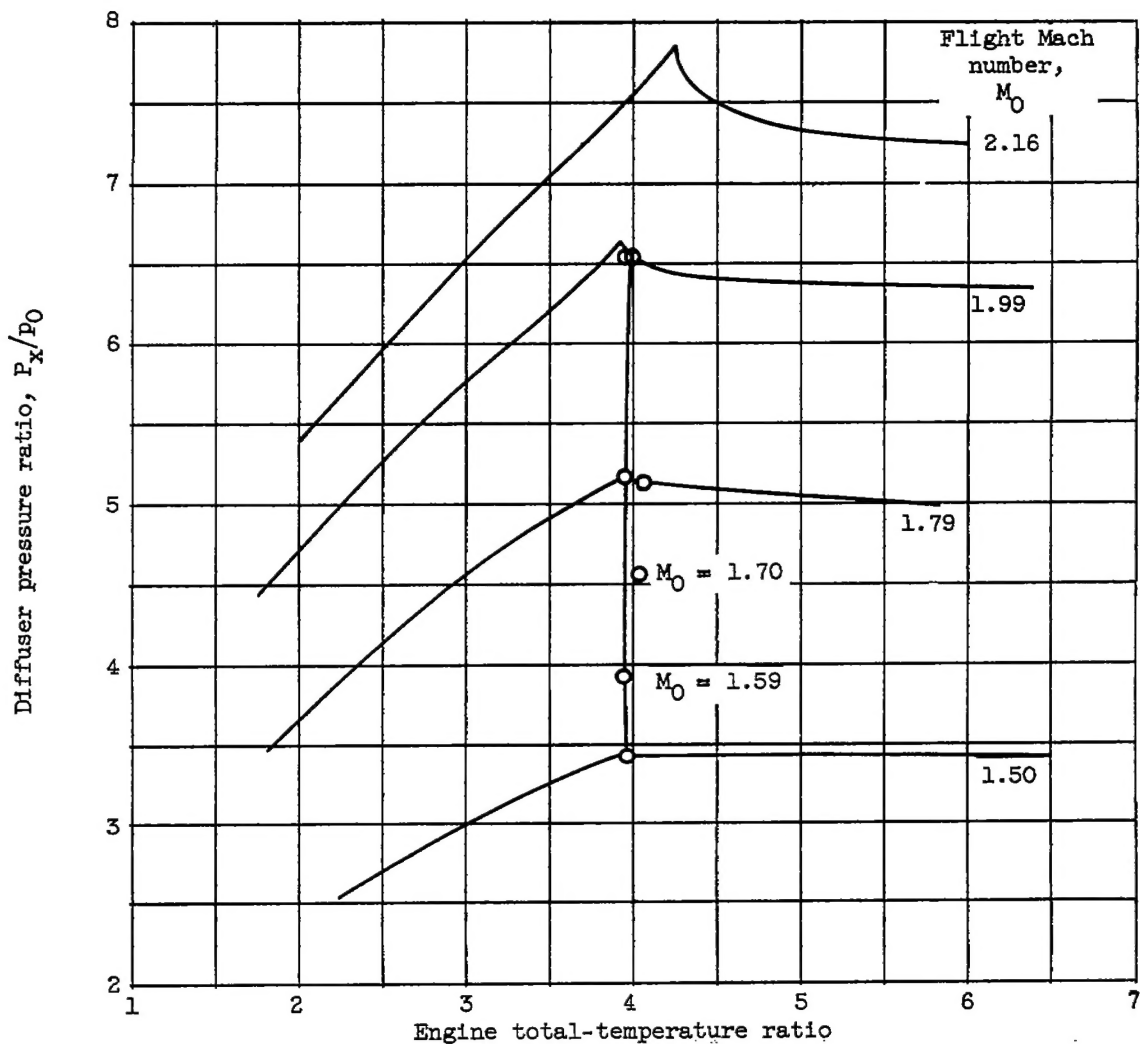


Figure 37. - Steady-state performance of optimalizing control of diffuser pressure. Engine-exit area  $A_6$ , 0.96 square foot; zero angle of attack.

CONFIDENTIAL

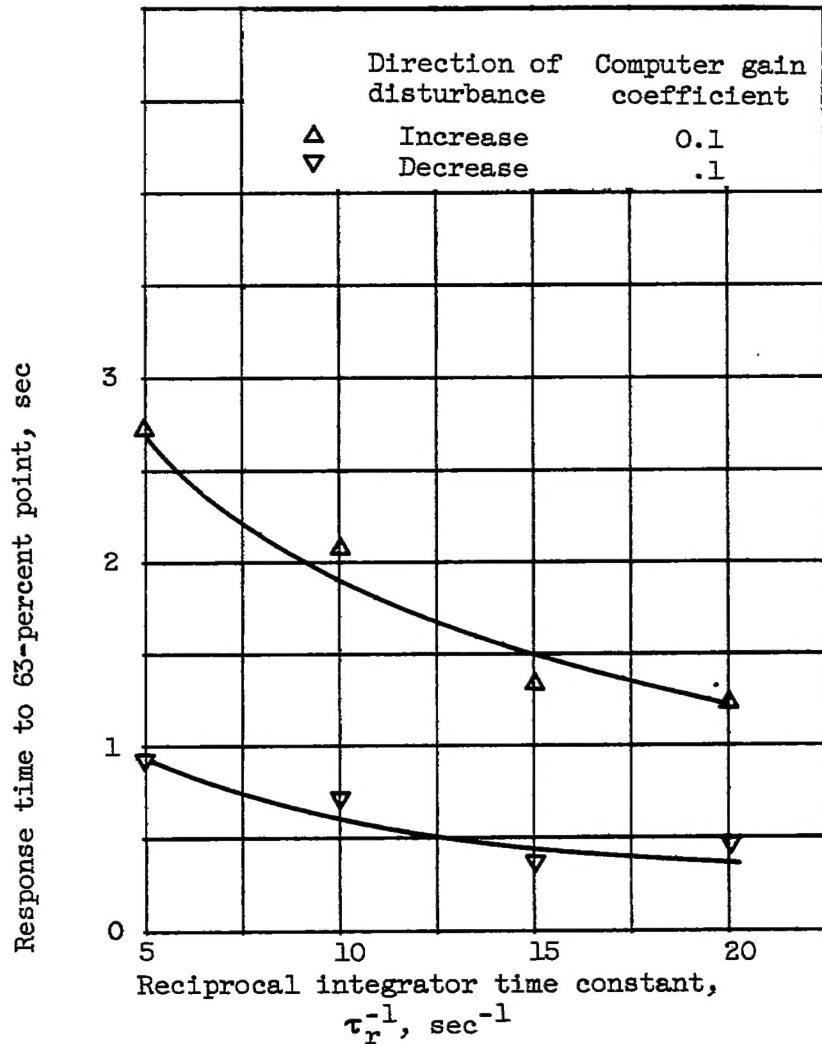


Figure 38. - Dynamic response of optimizer control. Response time as function of reciprocal integrator time constant. Flight Mach number  $M_0$ , 1.6; zero angle of attack; engine-exit area  $A_6$ , 0.96 square foot; fuel flow disturbance, 556 pounds per hour.

CONFIDENTIAL

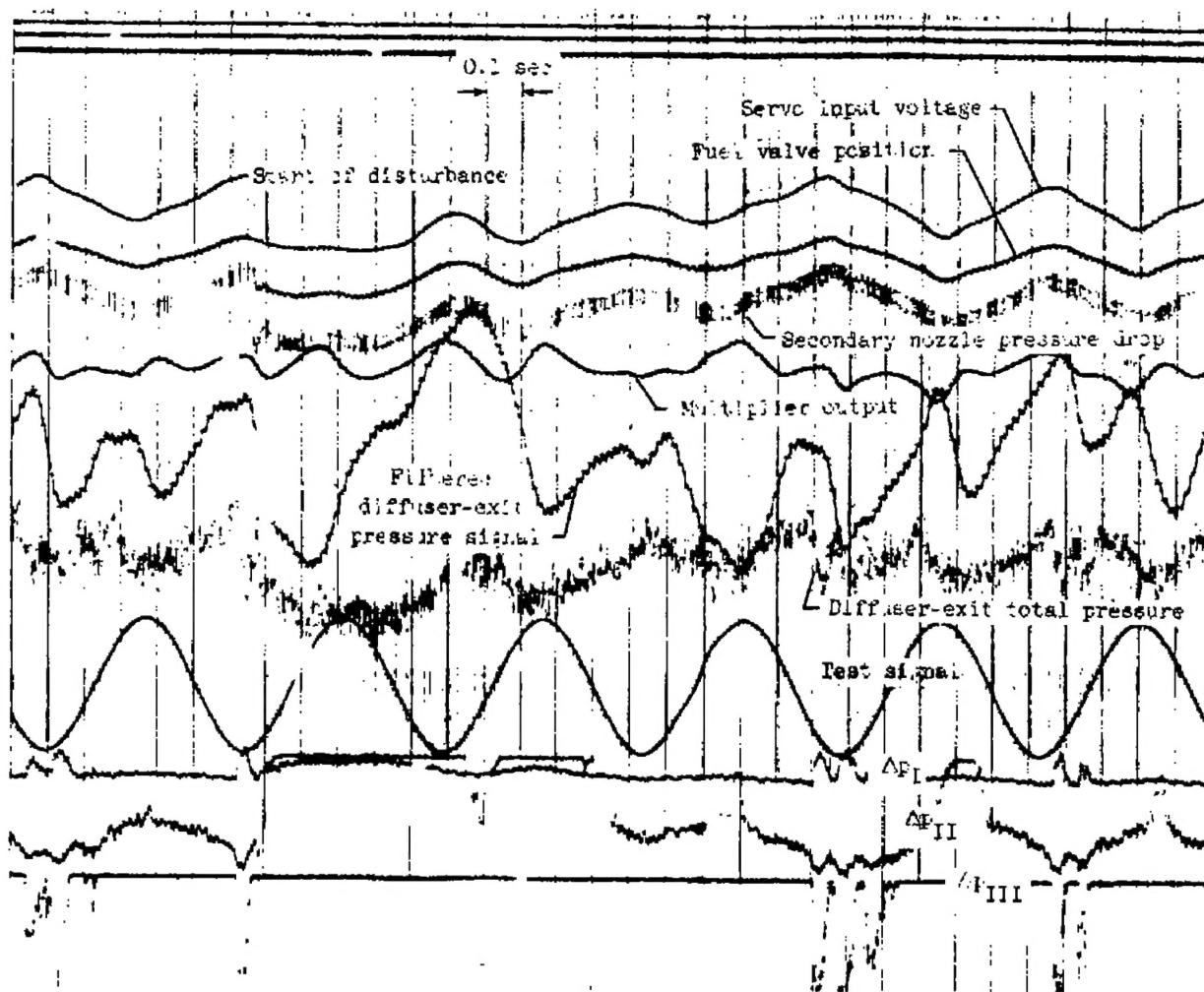


Figure 39. - Response of optimalizer control. Flight Mach number  $M_0$ , 2.0; zero angle of attack; fuel flow disturbance, -556 pounds per hour; computer gain, 0.05; control integrator time constant, 0.05 second.